iScience

CellPress
OPEN ACCESS

Article

Behavioral Teleporting of Individual Ethograms onto Inanimate Robots: Experiments on Social Interactions in Live Zebrafish

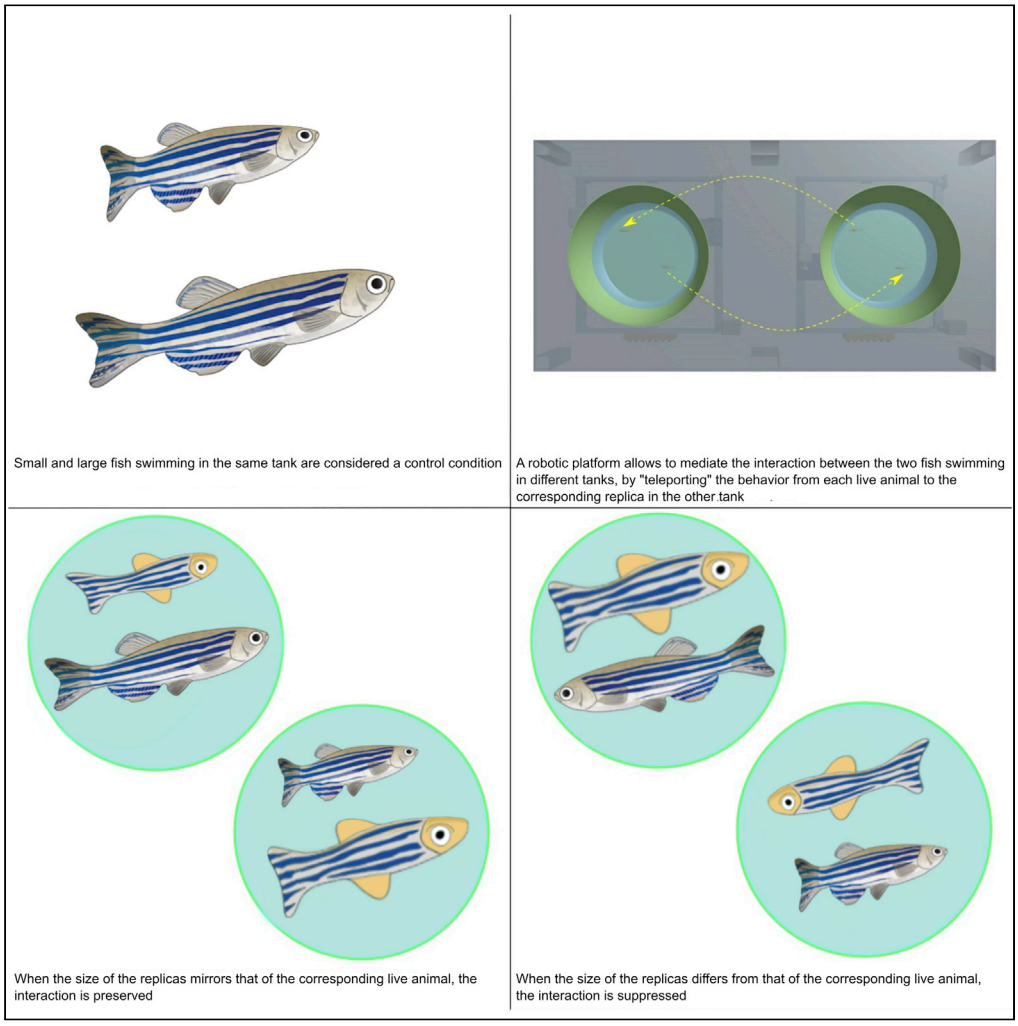

Mert Karakaya,
Simone Macrì,
Maurizio Porfiri

mporfiri@nyu.edu

HIGHLIGHTS

The ethogram of a live fish is transferred onto a remotely-located robotic replica

Social interactions of two zebrafish of different size are experimentally studied

Behavioral teleporting allows fine control over morphological features

The qualitative and quantitative nature of social interactions can be preserved

Karakaya et al., iScience *23*, 101418
August 21, 2020
https://doi.org/10.1016/j.isci.2020.101418

iScience

CellPress
OPEN ACCESS

Article

Behavioral Teleporting of Individual Ethograms onto Inanimate Robots: Experiments on Social Interactions in Live Zebrafish

Mert Karakaya,[1] Simone Macrì,[1,2] and Maurizio Porfiri[1,3,4,*]

SUMMARY

Social behavior is widespread in the animal kingdom, and it remarkably influences human personal and professional lives. However, a thorough understanding of the mechanisms underlying social behavior is elusive. Integrating the seemingly different fields of robotics and preclinical research could bring new insight on social behavior. Toward this aim, we established "behavioral teleporting" as an experimental solution to independently manipulate multiple factors underpinning social interactions. Behavioral teleporting consists of real-time transfer of the complete ethogram of a live zebrafish onto a remotely-located robotic replica. Through parallel and simultaneous behavioral teleporting, we studied the interaction between two live fish swimming in remotely-located tanks: each live fish interacted with an inanimate robot that mirrored the behavior of the other fish, and the morphology of each robot was independently tailored. Our results indicate that behavioral teleporting can preserve natural interaction between two live animals, while allowing fine control over morphological features that modulate social behavior.

INTRODUCTION

Social behavior determines the survival and reproductive success of many organisms (Choe, 2019). In humans, social behavior unfolds in actions, habits, and practices that ultimately define our individual life and our society (Bandura and Walters, 1977). Major deviations from societal norms often constitute symptoms of psychiatric disorders (autism [Lord et al., 2000] and schizophrenia [Buckner et al., 2008]). Inter-individual interactions are the outcome of complex processes, mediated by individual traits (genetic or environmental) and behavioral feedback that are often difficult to tease out from each other. For example, upon entering a meeting or approaching an unknown individual, we form strong biases within milliseconds (Naumann et al., 2009; Willis and Todorov, 2006). Factors like baldness, height, voice pitch, and outfit are likely to skew our consideration of other people (Nelissen and Meijers, 2011). As a result, behavioral feedback by our peers could have a very different effect, as a function of their appearance. How can we discriminate the effects of appearance and behavioral feedback? And, which visual features really matter?

Addressing these questions demands the isolation of the potential intervening variables through hypothesis-driven experiments. Laboratory animal studies represent one of the primary tools in this realm. Although rodents have traditionally constituted the taxa of choice, zebrafish are now emerging as a valid alternative (Macrì and Richter, 2015). This freshwater species is amenable to disentangling gene × environment interactions, whereby their genome is fully sequenced and modifiable through gene-editing procedures (Fontana et al., 2018; Kalueff et al., 2014). Likewise, pharmacological treatments targeting a given biological pathway are widely documented and procedurally standardized (Bao et al., 2019; de Abreu et al., 2019). Within the field of social interactions, zebrafish have been employed to investigate both normal behaviors and abnormal derailments (Meshalkina et al., 2018; Morris, 2009). Tang and collaborators (Tang et al., 2020) recently conducted a comprehensive study investigating the role of genes, putatively involved in human psychiatric disorders, in social behavior. Specifically, the authors tested 90 mutant lines against wild-type zebrafish and observed that the aforementioned mutations may alter the collective behavior of adult individuals. This study combined genetic engineering with a detailed automated phenotyping and advanced statistics to demonstrate that genetic manipulations map onto three identifiable patterns of collective behavior: group cohesion, alignment, and density. Yet, genetic engineering alone

[1]Department of Mechanical and Aerospace Engineering, New York University, Tandon School of Engineering, 6 MetroTech Center, Brooklyn, NY 11201, USA

[2]Centre for Behavioural Sciences and Mental Health, Istituto Superiore di Sanità, Viale Regina Elena 299, 00161 Rome, Italy

[3]Department of Biomedical Engineering, New York University, Tandon School of Engineering, 6 MetroTech Center, Brooklyn NY 11201, USA

[4]Lead Contact

*Correspondence: mporfiri@nyu.edu

https://doi.org/10.1016/j.isci.2020.101418

cannot provide the fine degree of control that is needed to determine the mechanism underlying social behavior.

For example, while addressing whether a specific gene or treatment (be it pharmacological or environmental) is involved in sociability, it is necessary to test how the experimental subject responds to a "standard" opponent. The "standard" nature of these opponents is far less than standardized—for rigorous scientific reasons. Standard opponents, in social interaction tests, may take the form of wild-type vehicle-treated control subjects (Kim et al., 2017; Liu et al., 2018) or subjects with a heterozygous background (Liu et al., 2018). Regardless of the selection of the most appropriate control group, even genetic manipulations per se may beget spurious phenotypes (Kim et al., 2017). Albeit extremely selective in nature, genetic manipulations have been shown to co-occur with off-target effects (genetic compensation), for which precise mechanisms have remained elusive (El-Brolosy and Stainier, 2017). Limited selectivity of the target phenotype extends beyond genetics, whereby the administration of psychoactive substances may influence many independent factors like locomotory patterns (Ladu et al., 2014), visual cues (Gerlai et al., 2000), and hormonal secretion (Sterling et al., 2015). Under these conditions, attributing the modulatory effects of a given drug on sociality to a specific underlying mechanism becomes questionable.

To isolate appearance from behavioral feedback in social interactions, several authors have proposed the integration of engineered, artificial stimuli in the form of visual playback or computer-animated images (Gerlai, 2010, 2014; Woo and Rieucau, 2011). Although these stimuli can attain a great degree of visual similarity, their locomotory patterns could inherently suffer from an imprecise representation of the real-life stimulus they were meant to resemble. The locomotion of visual images projected on computer screens is, by definition, constrained to the two-dimensional realm, which may fail to offer a realistic stimulus to live zebrafish. Recently, virtual reality has been explored as a powerful approach to create a rich, three-dimensional representation of the social environment (Naik et al., 2020; Stowers et al., 2017). Virtual reality overcomes several limitations of video playback and computer-animated images, by considerably enriching the repertoire of interactive behaviors that could be engineered and by improving the immersiveness of the experience by focal subjects. Besides coming at a considerable and potentially unaffordable cost that may challenge its widespread use in preclinical research, this approach still relies on projected images that may not fully capture the complexity of the three-dimensional stimulus of a live conspecific.

Biologically-inspired robots offer a promising alternative to virtual reality, by affording the delivery of physical, easily controllable, three-dimensional stimuli (Abdai et al., 2018; Frohnwieser et al., 2016; Porfiri, 2018; Romano et al., 2019). Yet, in comparison with virtual reality, robotics-based experimental setups do not allow an analogous level of controllability over morphological features and locomotory patterns. Additionally, it could be difficult to create an equivalently immersive experience through robotics-based setups, which are constrained by the practical limitations associated with any mechanical hardware. Despite these limitations, biologically-inspired robotic stimuli constitute faithful, three-dimensional representations of conspecifics in laboratory experiments on social behavior.

Although the initial efforts in this area were robotic stimuli that could only move along *a priori* determined trajectories, recent studies have demonstrated the possibility of interactive experiments with behavioral feedback (Bonnet et al., 2016; Cazenille et al., 2018; De Lellis et al., 2020; Kim et al., 2018; Kopman et al., 2013; Landgraf et al., 2013, 2016; Papaspyros et al., 2019). In all these interactive robotic platforms, an external manipulator is utilized to maneuver biologically-inspired replicas that interact with live animals on the basis of real-time feedback from an automated tracking system. The main difference among these robotic platforms is in the approach that is pursued to control the movements of the replica in response to the behavior of live animals. Some studies have proposed the integration of classical behavioral rules inspired by mathematical models of schooling and shoaling (Bonnet et al., 2016; Kim et al., 2018; Kopman et al., 2013; Landgraf et al., 2013, 2016), and others have employed recent data-driven stochastic models of fish behavior (De Lellis et al., 2020; Papaspyros et al., 2019) or alternative probability-based feedback mechanisms (Cazenille et al., 2018).

Notwithstanding their contribution to fundamental science and the corresponding level of technological sophistication, existing robotic platforms often lead to unnatural behavioral responses of live animals. We propose that this limited degree of biomimicry is associated with the common premise of all these approaches to use a mathematical representation of social behavior for controlling the movements of the

replica. To obviate the need of a mathematical representation of social behavior, we put forward the concept of "behavioral teleporting." Within behavioral teleporting, we transfer, in real time, the behavior of a live zebrafish onto the movements of a biologically-inspired replica located in another tank. The "copy/pasted" behavior of the live fish replaces the mathematical representation on which existing approaches are based.

Our concept of behavioral teleporting is related to two recent, independent breakthroughs by Bonnet and collaborators (Bonnet et al., 2019) and Larsch and Baier (Larsch and Baier, 2018). Bonnet and collaborators demonstrated the feasibility of remote interaction between zebrafish and honeybees in binary decision-making tasks through biologically-inspired robots (a zebrafish replica and two bee-robots). The authors showed that, by controlling the zebrafish replica through spatial density of honeybees and the bee-robot through the swimming direction of zebrafish, it was possible to establish a link between these two species. Larsch and Baier demonstrated the possibility of establishing remote social interactions between zebrafish within a virtual reality setup, wherein projected dots instantaneously replicated the motion of independent subjects located in different tanks. Our approach combines these two strategies by affording the transfer of the complete ethogram of a zebrafish, similar to Larsch and Baier (2018), onto a three-dimensional robotic replica, similar to Bonnet et al. (2019).

To validate the efficacy of our approach in the study of social interactions, we implemented behavioral teleporting in a setup consisting of two separate tanks, each containing one fish and one robotic replica (Figure 1A). An automated tracking system scored, in real time, the locomotory patterns of each of the live subjects, which were used to control the robotic replica swimming in the other tank. The complete ethogram of each fish was transferred across tanks within a fraction of a second, thereby establishing a complex robotics-mediated interaction between two remotely-located live animals.

The relevance of our approach to unveil the mechanism of social behavior was tested in an ethologically meaningful experiment, in which we systematically varied behavioral feedback and appearance (Figure 1B). We investigated whether behavioral teleporting would preserve the interaction between a large and a small fish, provided that the morphology of the robotic replicas resembled their live counterparts. To confirm this association, we manipulated the morphology of the replicas, such that a live subject would swim with a replica resembling a small but behaving like a large fish or looking large but behaving small (Figure 1C).

RESULTS

The Ethogram of a Live Zebrafish Can Be Transferred through Behavioral Teleporting

One of the primary aims of our work was to demonstrate the capability to transfer the motion of a live fish onto a robotic replica. To this end, we scored in real time the behavior of a live fish and, through an in-house developed robotic platform, we accordingly maneuvered a replica, located in a separate tank (Transparent Methods). Behavioral teleporting was always performed on two animals at the same time, thereby maneuvering two replicas at the same time. The extent to which a replica was successful in mirroring the motion of a live animal was assessed by cross-correlating their trajectories (Figure 2A). Experimental results indicate that the replica teleported the motion of the fish in almost all trials (85% of the total experimental time), with a 95% accuracy at a maximum time-lag smaller than 0.2 s (Figure 2B). The high accuracy in the replication of fish trajectory was confirmed by equivalent analysis on speed, turn rate, and acceleration (Text S1 and Figure S1).

In order to assess the feasibility of the developed system in hypothesis-driven experiments, we tested whether behavioral teleporting would preserve the simplest form of dyadic interaction between a large and small fish of the same sex (Figure 1C). Specifically, we compared the interaction between a small and a large fish swimming in the same tank against their remote interaction enabled by behavioral teleporting. In the Control condition, we scored the behavior of two live fish (one large and one small; average size difference of approximately 33%) of the same sex, swimming in the same tank for 10 min (Video S1). We pursued a within-subject experimental design, wherein the identity of every pair (12 pairs of fish of the same sex: six male pairs and six female pairs) was maintained across experimental conditions. Behavioral teleporting was implemented in the Match condition, where the same pairs tested in the Control condition were physically separated in two independent tanks. Within each tank, a fish of the pair swam with a conspecific-like replica matching the morphology and locomotory pattern of the fish located in the other

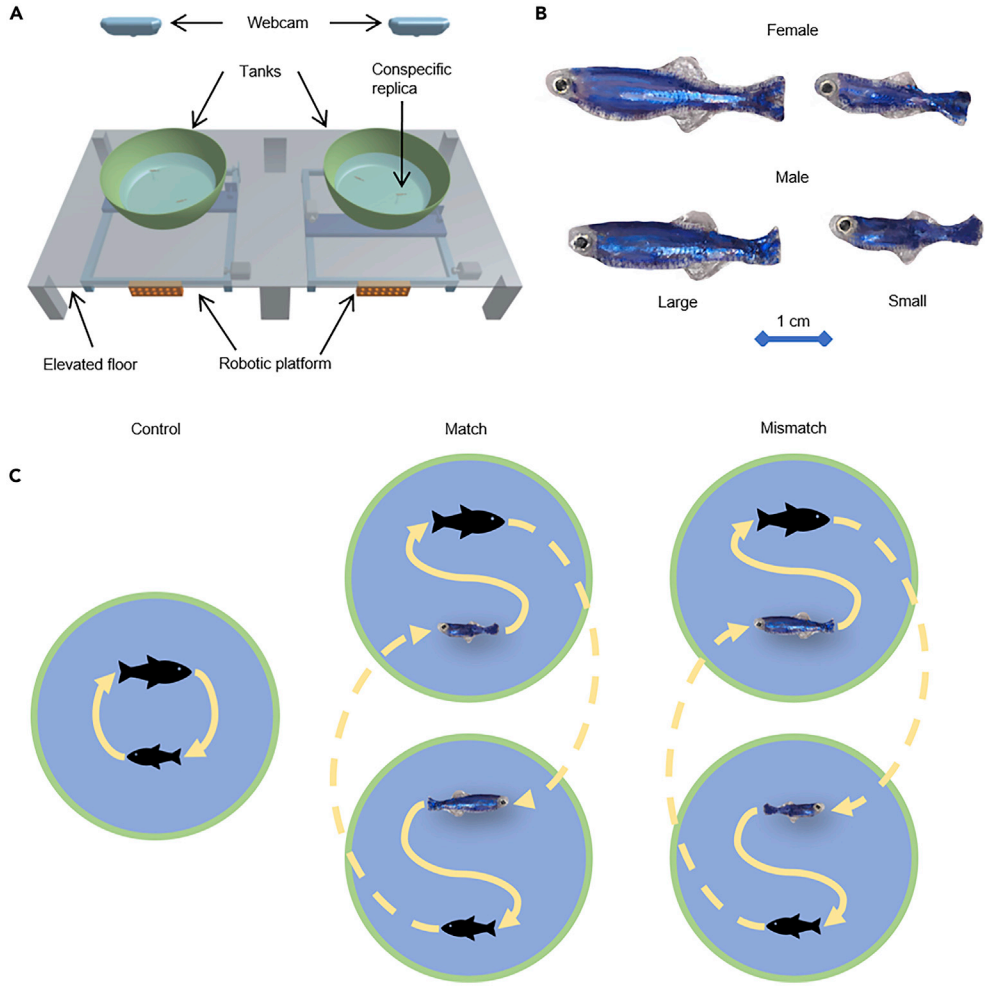

Figure 1. Experimental Setup and Conditions

Figure360▷ For a Figure360 author presentation of Figure, see https://doi.org/10.1016/j.isci.2020.101418.

(A) Experimental apparatus with two robotic platforms, two tanks, the base structure, and two overhead cameras.

(B) Female and male conspecific replicas of large and small sizes.

(C) Experimental conditions considered in our study: Control, Match, and Mismatch. The black cartoon fish represent live fish. Interactions within the same tank are highlighted through solid lines, whereas dashed lines indicate behavioral teleporting of a live fish onto a replica in a separate tank.

tank (Video S2). As a result, the large fish swam with a small replica that mirrored the locomotory patterns exhibited by the small fish positioned in the other tank, and vice versa.

Natural Patterns of Social Interactions Are Preserved in Match Condition

The interaction between the animals was scored through the information-theoretic notion of transfer entropy, which can be used to identify causal relationships between two systems in a Wiener-Granger sense (Bossomaier et al., 2016). We pursued a symbolic approach, in which we combined the time-series of the speed and turn rate to create a simplified, yet robust, representation of zebrafish ethogram. Four symbols were introduced based on the signs of the linear and angular accelerations; for example, one symbol described the case in which the speed of the fish decreased along with its turn rate. Computing transfer entropy between the symbolic time-series of the two fish in the same (Control condition) or different tanks (Match condition), we evaluated the extent to which knowledge about the behavior of one fish can improve the predictability of the future behavior of the other fish. Statistical significance was assessed through a non-parametric permutation test against a surrogate distribution of 20,000 randomly generated values. We expected to register transfer entropy values different from zero between the small and large fish in

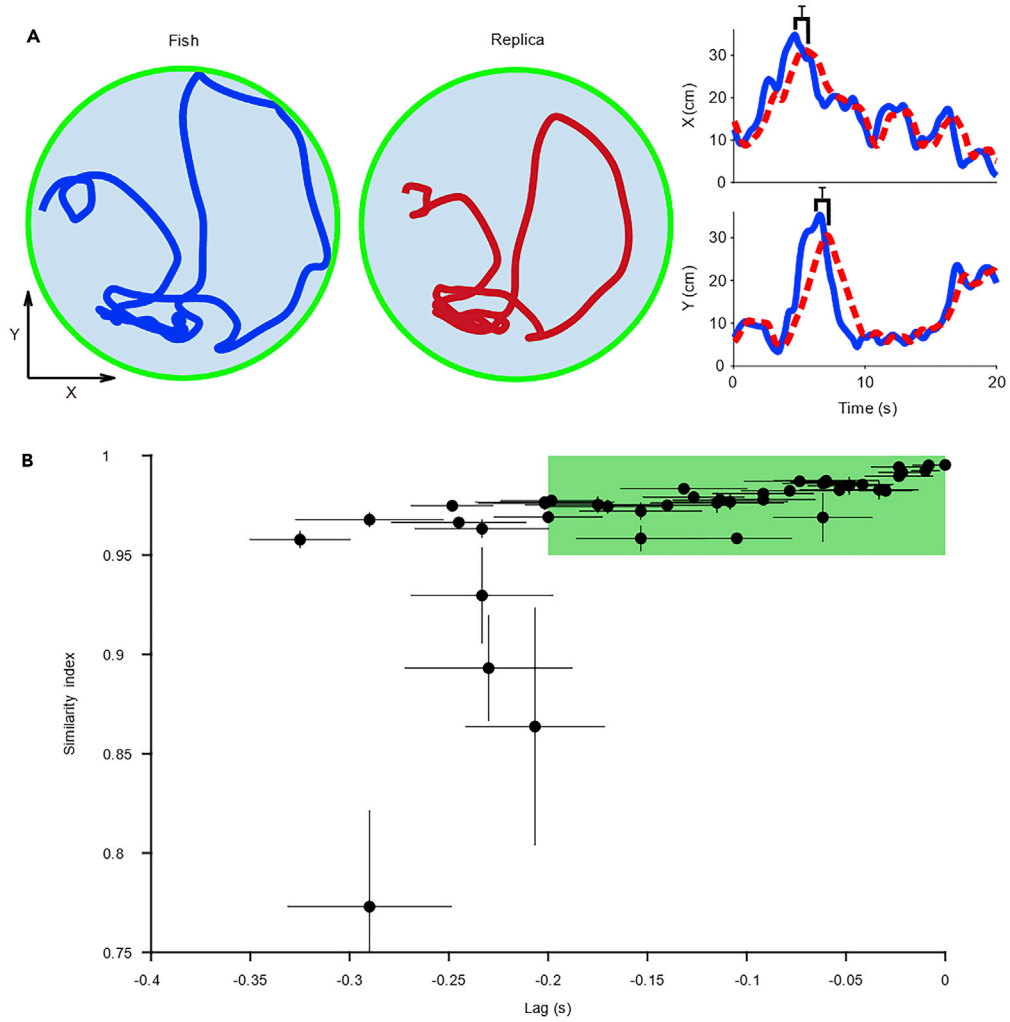

Figure 2. Performance of the Robotic Platform

(A) Left panel: trajectory of a small fish in Match condition over a 20-s time interval. Center panel: trajectory imposed on the small replica teleporting the behavior of the small fish in Match condition over the same time interval. Right panel: X and Y coordinates of the fish (blue line) and replica (dashed red line); brackets show the time-lag required to attain the maximum normalized cross-correlation (similarity index) between the replica and the fish.

(B) Similarity index as a function of the time-lag. For each experimental session, there are two circles that represent the averages of 30 similarity indices and corresponding time-lags. Whiskers represent standard deviations, and the green region identifies the range of successful experiments (22 trials/1,224 time intervals) in which the similarity index was above 0.95 within a time-lag of less than 0.2 s.

the Control condition, as they were allowed to swim in the same tank and mutually influence each other. Similarly, we predicted transfer entropy values different from zero in the Match condition, when the robotic replicas mediated the interaction between the subjects swimming in different tanks. Results in Table 1 confirm these predictions, pointing at a strong interaction between subjects swimming in the same or in different tanks ($p < 0.001$).

The robotic platform was not only successful in teleporting fish behavior across tanks and creating a remote interaction between subjects but also preserved the same relationship between small and large fish. We used net transfer entropy to quantify asymmetries in the pair, thereby detecting whether one of the two fish had a stronger influence on the other. In the Control condition, we observed that net transfer entropy was skewed toward the small fish ($p = 0.009$), thereby suggesting that the small had a stronger influence on the large than vice versa. The same skewness was preserved in the Match condition, wherein behavioral teleporting resulted in a stronger

	$TE_{Small \rightarrow Large}$	$TE_{Large \rightarrow Small}$	Net TE = $TE_{Small \rightarrow Large}$ - $TE_{Large \rightarrow Small}$
Control	6.504×10^{-3} (1.864×10^{-3}) $p < 0.001$	5.896×10^{-3} (1.619×10^{-3}) **$p < 0.001$**	6.073×10^{-4} (-2.076×10^{-4}; 4.313×10^{-4}) **$p = 0.009$**
Match	6.411×10^{-3} (1.935×10^{-3}) **$p < 0.001$**	5.012×10^{-3} (1.521×10^{-3}) **$p < 0.001$**	1.399×10^{-3} (-1.232×10^{-4}; 6.344×10^{-4}) **$p < 0.001$**
Mismatch	6.637×10^{-3} (2.169×10^{-3}) **$p < 0.001$**	6.828×10^{-3} (2.178×10^{-3}) **$p < 0.001$**	-1.901×10^{-4} (-3.837×10^{-4}; 3.855×10^{-4}) $p = 0.129$

Table 1. Synoptic Presentation of the Transfer Entropy Results on the Interaction between Small and Large Zebrafish as a Function of the Experimental Conditions

Transfer entropy analysis: average values, 95% (2.5% and 97.5%) quantiles from surrogate distributions for one-tailed (two-tailed) tests, and p values. Bold p values indicate significant results at a 5% significance level in permutation tests.

influence of the small fish on the large one swimming in a different tank ($p < 0.001$) (Figure 3). Delving into the qualitative nature of the asymmetric relationship between small and large fish, we investigated leader-follower relationships within the pair, following early work by Krause and collaborators who defined "leadership as the initiation of new directions of locomotion by one or more individuals which are then readily followed by other group members" (Krause et al., 2000). Within this realm, the fish that performed the first movement was considered the leader and the one that followed that movement was deemed a follower. We operationalized leader-follower interactions by computing cross-correlation on the time-series of either the speed or turn rate; an analogous approach to the quantification of leader-follower relationships has been used to study bird flocks (Nagy et al., 2010). For example, a leader would be defined as such if its accelerations or sudden turns were mirrored by the other fish (the follower). In practice, given one type of time-series (speed or turn rate), we computed the maximum value of the normalized cross-correlation and the corresponding time-lag. Although the value of the cross-correlation offers an indication of the strength of the interaction, the sign of the time-lag reveals which of the fish tends to lead the movement of the other (a positive value means that the small fish initiates movements that are followed by the large one, and a negative value refers to the opposite case). Similar to transfer entropy analysis, we assessed statistical significance through permutation tests against a surrogate distribution of 20,000 randomly generated values. We created a surrogate dataset by using the same approach as described for transfer entropy and analogously assessed statistical significance using a permutation test at 5% significance level.

With respect to speed in both Control and Match conditions, we registered values of normalized cross-correlation significantly larger than chance (normalized cross-correlation for Control and Match: 0.810 and 0.735, respectively; $p < 0.001$) with the small fish leading the large one significantly more often than chance (time-lag between small and large fish for Control and Match: 0.073 s and 0.057 s, respectively; $p < 0.001$) (Table 2). With respect to turn rate, Control subjects displayed value of the normalized cross-correlation significantly larger than chance (normalized cross-correlation: 0.241; $p < 0.001$), with the small fish leading the large one significantly more often than chance (time-lag between small and large fish: 0.077 s; $p < 0.001$) (Table 2). The same pattern was observed in Match subjects (time-lag between small and large fish: 0.037 s; $p = 0.010$), although the value of the normalized cross-correlation failed to reach statistical significance (normalized cross-correlation: 0.139; $p = 0.422$) (Table 2).

Natural Patterns of Social Interactions Are Altered in Mismatch Condition

To demonstrate that both morphology and locomotory patterns contribute to the relationship between the fish, we devised a condition in which the appearance of the replica was conflicting with its expected behavior. In this Mismatch condition, the behavior of a small fish was teleported onto a large replica swimming together with a large fish, whose behavior was, in turn, teleported onto a small replica swimming with the small fish (Figure 1C; Video S3). As mentioned above, the fish pairs identities were maintained

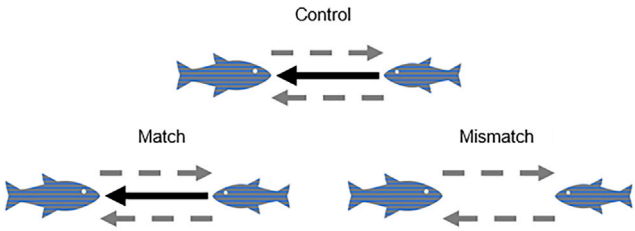

Figure 3. Graphical Representation of Significant Transfer Entropy Results across Conditions

Dashed gray arrows represent significant transfer entropy from one fish to the other, and the solid black line identifies significant net transfer entropy. In Control and Match conditions, the small fish influences the large one more than the other way around, whereas in Mismatch condition the interaction is not significantly skewed. Transfer entropy is computed on the basis of the time-series of the speed and turn rate (Figure 4).

throughout all conditions, so that the pairs tested in the Mismatch condition were the same as those tested in Control and Match conditions. Similar to Match condition, we registered a strong interaction between subjects swimming in the different tanks ($p < 0.001$) (Table 1). However, in accordance with our predictions, decoupling locomotory patterns from morphology abolished the asymmetry in the interaction, whereby net transfer entropy was undistinguishable from chance ($p = 0.129$) (Figure 3 and Table 1). It is important to emphasize that behavioral teleporting, together with the presence of replicas, did not influence general locomotion of live fish, whereby Control, Match, and Mismatch individuals exhibited indistinguishable values and temporal patterning of speed, turn rate, and acceleration, alongside with highly comparable spatial distribution in the experimental tank (Text S2 and Figures S2 and S3).

Delving into the qualitative nature of the interaction through cross-correlation analysis, we identified cross-correlation significantly larger than chance for both speed and turn rate (normalized cross-correlation: 0.744 and 0.142, respectively; $p < 0.001$ and $p = 0.003$, respectively) (Table 2). However, none of these interactions was explained by small or large fish systematically leading in the pair with respect to speed and turn rate (time-lag between small and large fish: −0.025 and 0.022 s, respectively; $p = 0.052$ and $p = 0.096$, respectively) (Table 2).

Shoaling and Schooling are affected by Behavioral Teleporting

Additional analyses on the qualitative interaction between the animals indicate that extent of schooling and shoaling tendency between subjects was reduced by behavioral teleporting (Text S2 and Figure S4). These reductions did not affect the ability of the approach to preserve natural interactions, whereby Control and Match subjects aligned their motion when in close proximity of a conspecific (Control) or a replica (Match), and such a relationship was not observed in the Mismatch condition (Text S2 and Figure S5).

DISCUSSION

In this paper, we designed and validated a robotics-based approach to perform hypothesis-driven experiments on zebrafish social behavior. Through the notion of behavioral teleporting, our approach enables fine control over locomotory patterns and morphological features of robotic stimuli. We demonstrated the possibility of transferring the behavior of a live animal onto a remotely-located robotic replica that consistently interacted with another live animal. Through parallel behavioral teleporting, we explored the interaction between two live zebrafish swimming in remotely-located tanks: each fish interacted with an inanimate robot which mirrored the locomotory patterns of the other subject.

Across all trials, we demonstrated the possibility of swiftly teleporting the behavior of live animals onto robotic replicas with a high degree of precision with respect to position, speed, turnrate, and acceleration. We believe that the efficacy of our platform was instrumental to the success of the present study. Previous endeavors in the field of interactive fish-robot interactions (Bonnet et al., 2016; Cazenille et al., 2018; De Lellis et al., 2020; Kim et al., 2018; Kopman et al., 2013; Landgraf et al., 2013, 2016; Papaspyros et al., 2019) have documented unexpected fish reactions to a robotic stimulus inspired by a conspecific. Our platform, instead, elicited the responses that should be predicted on the basis of fish-to-fish social behavior. This improved level of biomimicry should be attributed to the theoretical twist of this study, which embraces behavioral teleporting rather than mathematical representations of fish behavior. By obviating

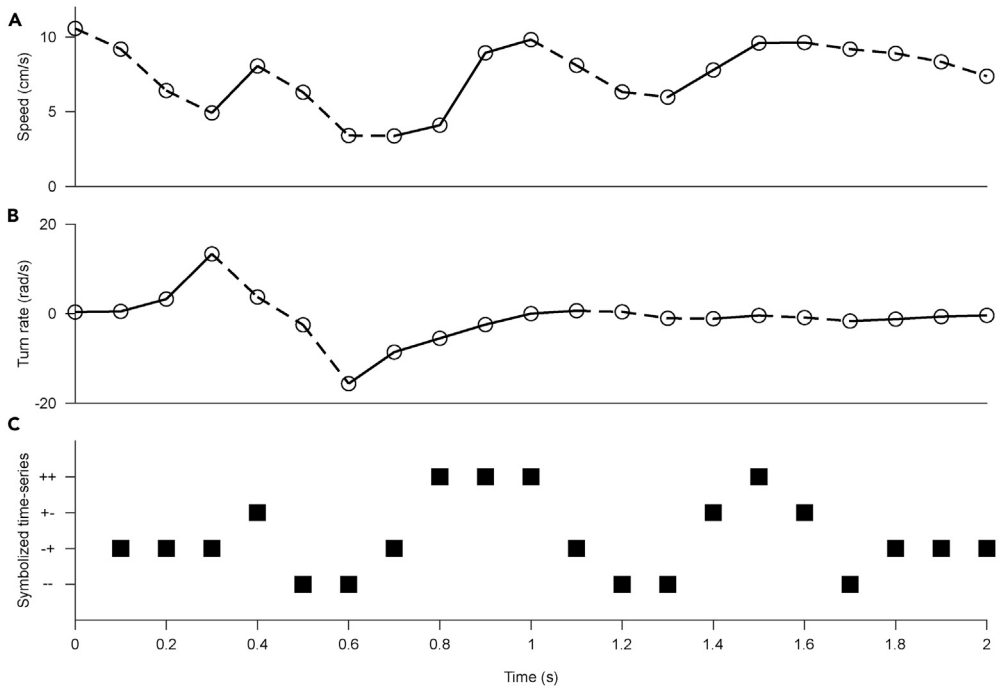

Figure 4. Joint Symbolization of Speed and Turn Rate

(A) Time-series of the speed of a fish within a 2-s window.

(B) Time-series of turn rate within the same window. Dashed and solid lines are associated with the decreasing and the increasing symbols, respectively.

(C) Joint symbolic time-series with four symbols ("–" decrease in speed and turn rate; "-+" decrease in speed and increase in turn rate, "+-" increase in speed and decrease in turn rate, and "++" increase in both speed and turn rate).

the need of a mathematical model to control the robotic stimulus, our methodology is devoid of any approximation that could skew the appraisal of the stimulus by the live animal. Our approach to maneuver the robotic replica does not rely on classical behavioral rules inspired by schooling and shoaling (Bonnet et al., 2016; Kim et al., 2018; Kopman et al., 2013; Landgraf et al., 2013, 2016), or on recent data-driven stochastic models of fish behavior (De Lellis et al., 2020; Papaspyros et al., 2019), or on probability-based feedback mechanisms (Cazenille et al., 2018).

The interaction between live animals swimming in the same or in different tanks was studied through the lens of information theory (Bossomaier et al., 2016). Specifically, we adopted the concept of transfer entropy (Schreiber, 2000) to quantify the extent to which the knowledge about the past behavior of one fish could reduce the uncertainty in predicting the behavior of the other fish from its past behavior. To increase statistical power, we opted for a symbolic representation (Staniek and Lehnertz, 2008) of the time-series of animal locomotion, where each symbol encoded a specific locomotory bout of the fish ethogram. In agreement with our expectations, we registered a strong mutual influence between the subjects in all experimental conditions (Control, Match, and Mismatch conditions). This finding demonstrates the feasibility of behavioral teleporting onto a replica to allow interaction between two remotely-located fish.

Upon such a robotics-mediated interaction, it is possible to devise hypothesis-driven experiments in which locomotory patterns must be faithfully reproduced by an inanimate robot and potentially dissociated from other intervening variables. The present experiments on the role of morphology in social behavior offer compelling evidence in favor of this proposition. Although coupling morphology with locomotory patterns during behavioral teleporting (Match condition) resulted in the preservation of the natural interaction between two live animals (Control condition), introducing a conflict between morphology and locomotory patterns (Mismatch condition) begot unnatural interactions. These manipulations are unprecedented in the field of animal-robot interactions, but they have roots in other fields of animal behavior. Extremely common in nature are instances of evolutionary-driven deceptions, in which an animal would change its

	Normalized Cross-Correlation of Speed	Time-Lag for Speed	Normalized Cross-Correlation of Turn Rate	Time-Lag for Turn Rate
Control	0.810 (0.767) **p < 0.001**	0.073 (−0.008; 0.042) **p < 0.001**	0.241 (0.168) **p < 0.001**	0.077 (−0.025; 0.049) **p < 0.001**
Match	0.735 (0.723) **p < 0.001**	0.057 (−0.018; 0.027) **p < 0.001**	0.139 (0.141) p = 0.422	0.037 (−0.028; 0.031) **p = 0.010**
Mismatch	0.744 (0.740) **p < 0.001**	−0.025 (−0.029; 0.014) p = 0.052	0.142 (0.140) **p = 0.003**	0.022 (−0.025; 0.033) p = 0.096

Table 2. Cross-Correlation Analysis on the Interaction between Small and Large Zebrafish for Different Experimental Conditions

Normalized cross-correlation and corresponding time-lags: average values 95% (2.5% and 97.5%) quantiles from surrogate distributions for one-tailed (two-tailed) tests, and p values. Bold p values indicate significant results at a 5% significance level in permutation tests.

behavior and appearance to mimic other conspecifics toward gaining some advantage. For example, in sexual mimicry, sneaky copulation is often pursued by small male fish that will mimic females to gain access to their female territory and enhance chances of copulation with them (Hanlon et al., 2005; Norman et al., 1999). Likewise, aggressive or defensive mimicry represents other instances of animals adopting traits that are not typical for their sex and age to improve their fitness (Randall, 2005).

The interaction between control subjects, which is preserved by behavioral teleporting in the Match condition, points at an asymmetric relationship between fish of different size. Specifically, transfer entropy from the small to the large fish is larger than transfer entropy from the large to the small fish, thereby denoting the small fish as the one driving the interaction. Delving into the qualitative nature of the interaction through cross-correlation analysis, we observed that the stronger influence of the small fish was explained by a tendency to initiate new maneuvers that were followed by the large fish. It is tenable that such an interaction could represent an instance of leader-follower relationship (Krause et al., 2000). The possibility of small fish leading larger individuals has already been documented in prior work on freshwater fish (Reebs, 2001), although conclusive evidence in favor of an association between leadership and body size is yet to be elucidated (Harris et al., 2010; Reebs, 2001; Ward et al., 2002).

One of the key findings of our study is that, in contrast with the Match condition, Mismatch subjects failed to replicate the large-to-small fish relationship observed in Control subjects. In the Mismatch condition, live fish swam together with replicas of their same size; yet, while the large replica replicated the behavior of the small fish, the small replica replicated the behavior of the large fish. Within this setting, we failed to observe the emergence of a robotics-mediated asymmetric interaction between the remotely-located fish. Additionally, animals did not display the natural tendency of aligning their swimming directions when they were in close proximity (Miller and Gerlai, 2012), which was registered in Control and Match conditions. Hence, any disruption in the association between locomotion and morphology can result in the lack of natural fish-to-fish relationships. This evidence strengthens the view that social dynamics depends on both locomotory patterns and morphological features, which could underlie the origins of leadership (King et al., 2009).

The approach presented herein opens several research avenues in preclinical models of physiology and disease. One of the main hurdles in preclinical research relates to the fact that behavior is inextricably linked to underlying endophenotypes, such as hormones, circadian rhythms, and gene expression. Hence, model subjects could present alterations that exceed the behavioral ones they were meant to present. For example, genetically modified or pharmacologically manipulated zebrafish may exhibit aberrant endophenotypes that could challenge fine control of experimental variables in the study of social behavior (Grossman et al., 2010; Kim et al., 2017). Ethanol may represent an epitome: its administration in zebrafish results in both behavioral (locomotion) (Ladu et al., 2014) and morphological (coloration) (Gerlai et al., 2000) alterations. Under these conditions, discriminating whether the influence of ethanol on sociality is mediated by behavior or morphology becomes impossible. Behavioral teleporting can help addressing this issue.

Limitations of the Study

In spite of anticipated advantages, our approach presents, nonetheless, several limitations. First and foremost, the locomotion of the replicas should be improved to reflect the complex behavioral repertoire of zebrafish in three dimensions. In the present study, to demonstrate the feasibility of our approach, experimental subjects (and replicas) were constrained to shallow water, thereby preventing the onset of complex species-specific three-dimensional trajectories (Kalueff et al., 2013). Although this decision was functional to the scopes of our study, we acknowledge that future incarnations shall contemplate three-dimensional behavioral teleporting and scoring. This main hurdle depends on both the computational load necessary to reconstruct three-dimensional trajectories of live fish and, most importantly, hardware requirements to design untethered robotic stimuli that could autonomously swim along three-dimensional trajectories.

Another key aspect to be improved is in the extent of biological mimicry. Although the replicas we devised allowed preserving several aspects of the interactions between live animals swimming in the same tank, they nonetheless failed to maintain the same absolute values of shoaling and schooling tendencies registered in Control subjects. A number of factors might contribute to this limitation, including incomplete replication of body undulations through mere passive compliance, imperfect pigmentation and stripe patterning, lack of moving fins and gills, absence of olfactory cues similar to live animals, and undesired mechanical vibrations from the robotic platform. All these factors are in fact known to contribute to the appraisal of other fish by zebrafish individuals (Engeszer et al., 2004, 2008; Polverino et al., 2012; Rosenthal and Ryan, 2005; Saverino and Gerlai, 2008; Yoshihara, 2014).

Another potential limitation of this study relates to the selection of control subjects. Specifically, resting upon the objective to investigate the effect of differential body size, we conducted the study on subjects characterized by major differences in body length. This resulted in a fish population consisting of large and small individuals. Having two "extreme" populations did not allow resolution of the absolute effect of body size, whereby we lacked a subject of intermediate size that could represent a reference comparison. Future studies could involve a larger fish population, in which one could examine robotics-mediated interaction between remotely-located live animals of small and intermediate sizes as well as animals of large and intermediate sizes.

Resource Availability

Lead Contact

Further information and requests for resources should be directed to and will be fulfilled by the Lead Contact, Maurizio Porfiri (mporfiri@nyu.edu).

Materials Availability

This study did not generate any materials.

Data and Code Availability

Datasets and MATLAB scripts can be downloaded from the GitHub repository of the Dynamical Systems Laboratory at New York University: https://github.com/dynamicalsystemslaboratory/BehavioralTeleporting.

METHODS

All methods can be found in the accompanying Transparent Methods supplemental file.

SUPPLEMENTAL INFORMATION

Supplemental Information can be found online at https://doi.org/10.1016/j.isci.2020.101418.

ACKNOWLEDGMENTS

The authors are grateful to Romain J. G. Clement for his help in formulating the approach and participating in pilot experiments, to Hua Fang Lee for his assistance in developing a first prototype of the platform, and to Emanuela Grillo for her help with the graphical abstract.

This work was supported by the National Science Foundation under grant number CMMI-1505832, by the National Institutes of Health, National Institute on Drug Abuse under grant number 1R21DA042558-01A1, and by the Office of Behavioral and Social Sciences Research that co-funded the National Institute on Drug Abuse grant.

AUTHOR CONTRIBUTIONS

Conceptualization, M.K. and M.P.; Methodology, M.K., S.M., and M.P.; Software, M.K.; Validation, M.K., S.M., and M.P.; Formal Analysis, M.K., S.M., and M.P.; Investigation, M.K., S.M., and M.P.; Data Curation, M.K.; Writing - Original Draft, M.K., S.M., and M.P.; Writing - Review & Editing Draft, S.M. and M.P.; Visualization, M.K.; Supervision, M.P.; Project Administration, M.P.; Funding Acquisition, S.M. and M.P.

DECLARATION OF INTERESTS

The authors declare no competing interests.

Received: April 25, 2020
Revised: June 11, 2020
Accepted: July 26, 2020
Published: August 21, 2020

REFERENCES

Abdai, J., Korcsok, B., Korondi, P., and Miklósi, A. (2018). Methodological challenges of the use of robots in ethological research. Anim. Behav. Cogn. *5*, 326–340.

Bandura, A., and Walters, R.H. (1977). Social learning theory. In Englewood Cliffs, Vol. 1, (NJ: Prentice-hall). http://www.asecib.ase.ro/mps/Bandura_SocialLearningTheory.pdf.

Bao, W., Volgin, A.D., Alpyshov, E.T., Friend, A.J., Strekalova, T.V., de Abreu, M.S., Collins, C., Amstislavskaya, T.G., Demin, K.A., and Kalueff, A.V. (2019). Opioid neurobiology, neurogenetics and neuropharmacology in zebrafish. Neuroscience *404*, 218–232.

Bonnet, F., Kato, Y., Halloy, J., and Mondada, F. (2016). Infiltrating the zebrafish swarm: design, implementation and experimental tests of a miniature robotic fish lure for fish–robot interaction studies. Artif. Life Robot. *21*, 239–246.

Bonnet, F., Mills, R., Szopek, M., Schönwetter-Fuchs, S., Halloy, J., Bogdan, S., Correia, L., Mondada, F., and Schmickl, T. (2019). Robots mediating interactions between animals for interspecies collective behaviors. Sci. Robot. *4*, eaau7897.

Bossomaier, T., Barnett, L., Harré, M., and Lizier, J.T. (2016). An Introduction to Transfer Entropy (Springer International Publishing), pp. 65–95.

Buckner, R.L., Andrews-Hanna, J.R., and Schacter, D.L. (2008). The brain's default network: anatomy, function, and relevance to disease. Ann. New York Acad. Sci. *1124*, 1–38.

Cazenille, L., Chemtob, Y., Bonnet, F., Gribovskiy, A., Mondada, F., Bredeche, N., and Halloy, J. (2018). How to blend a robot within a group of zebrafish: achieving social acceptance through real-time calibration of a multi-level behavioural model. Paper presented at: Conference on Biomimetic and Biohybrid Systems (Springer).

Choe, J.C. (2019). Encyclopedia of Animal Behavior, 2nd edn (Academic Press).

de Abreu, M.S., Giacomini, A.C., Genario, R., Dos Santos, B.E., da Rosa, L.G., Demin, K.A., Wappler-Guzzetta, E., and Kalueff, A.V. (2019). Neuropharmacology, pharmacogenetics and pharmacogenomics of aggression: the zebrafish model. Pharmacol. Res. *141*, 602–608.

De Lellis, P., Cadolini, E., Croce, A., Yang, Y., di Bernardo, M., and Porfiri, M. (2020). Model-based feedback control of live zebrafish behavior via interaction with a robotic replica. IEEE Trans. Robot. *36*, 28–41.

El-Brolosy, M.A., and Stainier, D.Y. (2017). Genetic compensation: a phenomenon in search of mechanisms. PLoS Genet. *13*, e1006780.

Engeszer, R.E., Ryan, M.J., and Parichy, D.M. (2004). Learned social preference in zebrafish. Curr. Biol. *14*, 881–884.

Engeszer, R.E., Wang, G., Ryan, M.J., and Parichy, D.M. (2008). Sex-specific perceptual spaces for a vertebrate basal social aggregative behavior. Proc. Natl. Acad. Sci. U S A *105*, 929–933.

Fontana, B.D., Mezzomo, N.J., Kalueff, A.V., and Rosemberg, D.B. (2018). The developing utility of zebrafish models of neurological and neuropsychiatric disorders: a critical review. Exp. Neurol. *299*, 157–171.

Frohnwieser, A., Murray, J.C., Pike, T.W., and Wilkinson, A. (2016). Using robots to understand animal cognition. J. Exp. Anal. Behav. *105*, 14–22.

Gerlai, R. (2010). High-throughput behavioral screens: the first step towards finding genes involved in vertebrate brain function using zebrafish. Molecules *15*, 2609–2622.

Gerlai, R. (2014). Social behavior of zebrafish: from synthetic images to biological mechanisms of shoaling. J. Neurosci. Methods *234*, 59–65.

Gerlai, R., Lahav, M., Guo, S., and Rosenthal, A. (2000). Drinks like a fish: zebra fish (*Danio rerio*) as a behavior genetic model to study alcohol effects. Pharmacol. Biochem. Behav. *67*, 773–782.

Grossman, L., Utterback, E., Stewart, A., Gaikwad, S., Chung, K.M., Suciu, C., Wong, K., Elegante, M., Elkhayat, S., and Tan, J. (2010). Characterization of behavioral and endocrine effects of LSD on zebrafish. Behav. Brain Res. *214*, 277–284.

Hanlon, R.T., Naud, M.-J., Shaw, P.W., and Havenhand, J.N. (2005). Transient sexual mimicry leads to fertilization. Nature *433*, 212.

Harris, S., Ramnarine, I.W., Smith, H.G., and Pettersson, L.B. (2010). Picking personalities apart: estimating the influence of predation, sex and body size on boldness in the guppy *Poecilia reticulata*. Oikos *119*, 1711–1718.

Kalueff, A.V., Echevarria, D.J., and Stewart, A.M. (2014). Gaining translational momentum: more zebrafish models for neuroscience research. Prog. Neuro Psychopharmacol. Biol. Psychiatry *55*, 1–6.

Kalueff, A.V., Gebhardt, M., Stewart, A.M., Cachat, J.M., Brimmer, M., Chawla, J.S., Craddock, C., Kyzar, E.J., Roth, A., and Landsman, S. (2013). Towards a comprehensive catalog of zebrafish behavior 1.0 and beyond. Zebrafish *10*, 70–86.

Kim, C., Ruberto, T., Phamduy, P., and Porfiri, M. (2018). Closed-loop control of zebrafish behaviour in three dimensions using a robotic stimulus. Sci. Rep. *8*, 657.

Kim, O.-H., Cho, H.-J., Han, E., Hong, T.I., Ariyasiri, K., Choi, J.-H., Hwang, K.-S., Jeong, Y.-M., Yang, S.-Y., and Yu, K. (2017). Zebrafish knockout of Down syndrome gene, DYRK1A, shows social impairments relevant to autism. Mol. Autism *8*, 50.

King, A.J., Johnson, D.D., and Van Vugt, M. (2009). The origins and evolution of leadership. Curr. Biol. *19*, R911–R916.

Kopman, V., Laut, J., Polverino, G., and Porfiri, M. (2013). Closed-loop control of zebrafish response using a bioinspired robotic-fish in a preference test. J. R. Soc. Interf. *10*, 20120540.

Krause, J., Hoare, D., Krause, S., Hemelrijk, C., and Rubenstein, D. (2000). Leadership in fish shoals. Fish Fish. *1*, 82–89.

Ladu, F., Butail, S., Macrí, S., and Porfiri, M. (2014). Sociality modulates the effects of ethanol in zebra fish. Alcohol. Clin. Exp. Res. *38*, 2096–2104.

Landgraf, T., Bierbach, D., Nguyen, H., Muggelberg, N., Romanczuk, P., and Krause, J. (2016). RoboFish: increased acceptance of interactive robotic fish with realistic eyes and natural motion patterns by live Trinidadian guppies. Bioinspir. Biomim. *11*, 015001.

Landgraf, T., Nguyen, H., Forgo, S., Schneider, J., Schröer, J., Krüger, C., Matzke, H., Clément, R.O., Krause, J., and Rojas, R. (2013). Interactive robotic fish for the analysis of swarm behavior. Paper presented at: International Conference in Swarm Intelligence (Springer).

Larsch, J., and Baier, H. (2018). Biological motion as an innate perceptual mechanism driving social affiliation. Curr. Biol. *28*, 3523–3532.e4.

Liu, C.-X., Li, C.-Y., Hu, C.-C., Wang, Y., Lin, J., Jiang, Y.-H., Li, Q., and Xu, X. (2018). CRISPR/Cas9-induced shank3b mutant zebrafish display autism-like behaviors. Mol. Autism *9*, 23.

Lord, C., Risi, S., Lambrecht, L., Cook, E.H., Leventhal, B.L., DiLavore, P.C., Pickles, A., and Rutter, M. (2000). The autism diagnostic observation schedule—generic: a standard measure of social and communication deficits associated with the spectrum of autism. J. Autism Dev. Disord. *30*, 205–223.

Macrì, S., and Richter, S.H. (2015). The snark was a boojum-reloaded. Front. Zoolog. *12*, S20.

Meshalkina, D.A., Kizlyk, M.N., Kysil, E.V., Collier, A.D., Echevarria, D.J., Abreu, M.S., Barcellos, L.J., Song, C., Warnick, J.E., and Kyzar, E.J. (2018). Zebrafish models of autism spectrum disorder. Exp. Neurol. *299*, 207–216.

Miller, N., and Gerlai, R. (2012). From schooling to shoaling: patterns of collective motion in zebrafish (*Danio rerio*). PLoS One *7*, e48865.

Morris, J.A. (2009). Zebrafish: a model system to examine the neurodevelopmental basis of schizophrenia. In Progress in Brain Research (Elsevier), pp. 97–106.

Nagy, M., Ákos, Z., Biro, D., and Vicsek, T. (2010). Hierarchical group dynamics in pigeon flocks. Nature *464*, 890–893.

Naik, H., Bastien, R., Navab, N., and Couzin, I. (2020). Animals in virtual environments. IEEE Trans. Vis. Comput. Graph. *26*, 2073–2083.

Naumann, L.P., Vazire, S., Rentfrow, P.J., and Gosling, S.D. (2009). Personality judgments based on physical appearance. Personal. Soc. Psychol. Bull. *35*, 1661–1671.

Nelissen, R.M., and Meijers, M.H. (2011). Social benefits of luxury brands as costly signals of wealth and status. Evol. Hum. Behav. *32*, 343–355.

Norman, M.D., Finn, J., and Tregenza, T. (1999). Female impersonation as an alternative reproductive strategy in giant cuttlefish. Proc. R. Soc. Lond. Ser. B Biol. Sci. *266*, 1347–1349.

Papaspyros, V., Bonnet, F., Collignon, B., and Mondada, F. (2019). Bidirectional interactions facilitate the integration of a robot into a shoal of zebrafish danio rerio. PLoS One *14*, e0220559.

Polverino, G., Abaid, N., Kopman, V., Macrì, S., and Porfiri, M. (2012). Zebrafish response to robotic fish: preference experiments on isolated individuals and small shoals. Bioinspir. Biomim. *7*, 036019.

Porfiri, M. (2018). Inferring causal relationships in zebrafish-robot interactions through transfer entropy: a small lure to catch a big fish. Anim. Behav. Cogn. *5*, 341–367.

Randall, J.E. (2005). A review of mimicry in marine fishes. Zoolog. Stud. *44*, 299.

Reebs, S.G. (2001). Influence of body size on leadership in shoals of golden shiners, *Notemigonus crysoleucas*. Behaviour *138*, 797–809.

Romano, D., Donati, E., Benelli, G., and Stefanini, C. (2019). A review on animal–robot interaction: from bio-hybrid organisms to mixed societies. Biol. Cybernetics *113*, 201–225.

Rosenthal, G.G., and Ryan, M.J. (2005). Assortative preferences for stripes in danios. Anim. Behav. *70*, 1063–1066.

Saverino, C., and Gerlai, R. (2008). The social zebrafish: behavioral responses to conspecific, heterospecific, and computer animated fish. Behav. Brain Res. *191*, 77–87.

Schreiber, T. (2000). Measuring information transfer. Phys. Rev. Lett. *85*, 461.

Staniek, M., and Lehnertz, K. (2008). Symbolic transfer entropy. Phys. Rev. Lett. *100*, 158101.

Sterling, M., Karatayev, O., Chang, G.-Q., Algava, D., and Leibowitz, S. (2015). Model of voluntary ethanol intake in zebrafish: effect on behavior and hypothalamic orexigenic peptides. Behav. Brain Res. *278*, 29–39.

Stowers, J.R., Hofbauer, M., Bastien, R., Griessner, J., Higgins, P., Farooqui, S., Fischer, R.M., Nowikovsky, K., Haubensak, W., Couzin, I.D., et al. (2017). Virtual reality for freely moving animals. Nat. Methods *14*, 995.

Tang, W., Davidson, J.D., Zhang, G., Conen, K.E., Fanga, J., Serluca, F., Li, J., Xiong, X., Coble, M., and Tsai, T. (2020). Genetic control of collective behavior in zebrafish. iScience *23*, 100942.

Ward, A.J., Hoare, D.J., Couzin, I.D., Broom, M., and Krause, J. (2002). The effects of parasitism and body length on positioning within wild fish shoals. J. Anim. Ecol. *71*, 10–14.

Willis, J., and Todorov, A. (2006). First impressions: making up your mind after a 100-ms exposure to a face. Psychol. Sci. *17*, 592–598.

Woo, K.L., and Rieucau, G. (2011). From dummies to animations: a review of computer-animated stimuli used in animal behavior studies. Behav. Ecol. Sociobiol. *65*, 1671.

Yoshihara, Y. (2014). Zebrafish olfactory system. In The Olfactory System, K. Mori, ed. (Springer), pp. 71–96.

iScience, Volume *23*

Supplemental Information

Behavioral Teleporting of Individual Ethograms onto Inanimate Robots: Experiments on Social Interactions in Live Zebrafish

Mert Karakaya, Simone Macrì, and Maurizio Porfiri

Supplemental information

Text S1. Performance of the robotic platform, related to Figure 2

In addition to the similarity index considered in the main document, we examined the performance of the platform by comparing the speed, turn rate, and magnitude of the acceleration of the replica to a live fish. Specifically, we conducted a cross-correlation analysis, equivalent to the one explained in the main document, for all of these metrics. We limited the analysis to the 20-s time-intervals that were deemed successful in terms of the similarity index. For each interval, we computed the maximum value of the normalized cross-correlation and the corresponding time-lag. Different from the main document, we extended the range of admissible time-lags to 0.4 s, to acknowledge the numerical differentiation required in the calculation of speed, acceleration, and turn rate. We calculated a total of 1018 values of the maximum cross-correlation values for speed, turn rate, and magnitude of the acceleration with averages (standard errors) of 0.919 (± 0.002), 0.730 (± 0.003), and 0.849 (± 0.002), respectively (Fig. S1).

Text S2. Additional spatio-temporal analysis of live fish behavior, related to Figure 3 and Table 1

To investigate the behavioral similarity among the three experimental groups, we assessed speed, turn rate, and the magnitude of the acceleration in large and small fish tested in Control, Match, and Mismatch conditions. These data were analyzed through repeated measures ANOVA for split-plot designs with one between-subject factor (size: large versus small) and two within-subject factors (condition: Control versus Match versus Mismatch; time-bins: five 2-min intervals). For Match and Mismatch conditions, we limited the analysis to the 20-s time-intervals that were deemed to be successful by the similarity index described in the main document.

From our analysis, we conclude that speed was comparable between large and small individuals ($F_{1,18}$=1.68, p=0.212; Fig. S2A,B). While experimental groups apparently swam at a different speed ($F_{2,36}$=3.54, p=0.039; Fig. S2A,B), post-hoc comparisons failed to identify significant pairwise differences between conditions. Likewise, we recorded a variation of the speed over time ($F_{4,36}$=4.61, p=0.002; Fig. S2A,B); post-hoc analyses revealed that speed was higher between minutes 3-6 than 9-10 (p<0.05; Fig. S2A,B). With respect to turn rate, neither did we register a difference with respect to the size of the animals ($F_{1,18}$=0.68, p=0.420; Fig. S2C,D), nor with respect to the experimental condition ($F_{2,36}$=0.60, p=0.555; Fig. S2C,D). The magnitude of the turn rate changed over time ($F_{4,36}$=32.03, p<0.001; Fig. S2C,D), with post-hoc pairwise comparisons indicating a decline from minutes 1-2 to 9-10 (p<0.05; Fig. S2C,D). The analysis of the acceleration magnitude paralleled that of the speed, whereby we did not register an effect of size ($F_{1,18}$=1.51, p=0.235; Fig. S2E,F) and differences in conditions ($F_{2,36}$=4.75, p=0.015; Fig. S2E,F) did not translate into significant pairwise comparisons. The acceleration magnitude varied in time ($F_{4,36}$=16.54, p<0.001; Fig. S2E,F), all animals exhibiting higher acceleration during the early stage of the experimental session than towards the end (p<0.05; Fig. S2E,F). Alongside with analysis of general locomotion, we examined the spatial distribution of all the animals across experimental conditions, confirming equivalent response of each animal when tested with another conspecific or a replica through behavioral teleporting (Fig. S3).

In addition to examining temporal and spatial patterning of swimming activity, we analyzed the extent to which fish pairs coordinated their motion across experimental conditions in terms of schooling and shoaling (Miller and Gerlai, 2012; Tunstrøm et al., 2013). The analysis of robotics-mediated interactions of remotely-located fish in Match and Mismatch conditions was performed by using local reference frames in each tank. In practical terms, the trajectories of the fish in the two different tanks were superimposed on the same reference frame. Similar to the main text and the analysis presented above, for Match and Mismatch conditions, we only considered the 20-s time-intervals in which the platform performed as expected. We used a repeated measures ANOVA with two within-subject factors (condition: Control versus Match versus Mismatch; time-bins: five 2-min intervals). Tukey's honestly significant different (HSD) post-hoc tests were used when allowed. Statistical significance was set at 5%.

To quantify schooling tendency, we utilized polarization (Miller and Gerlai, 2012; Tunstrøm et al., 2013), which measures the extent to which fish aligned their orientation (Fig. S4A). Polarization varies between zero and one, where 1 indicates fully coordinated swimming with both fish swimming in the same direction. Highly coordinated swimming was observed in the Control condition, with an average polarization of 0.725. In the Match and Mismatch conditions, average polarizations of 0.635 and 0.640 were observed, respectively. Such a difference between Control individuals and subjects in Match and Mismatch conditions was confirmed by statistical analysis ($F_{2,18}$=25.67, p<0.001; p<0.05 in post-hoc tests; Fig. S4A) and was consistent over time ($F_{4,36}$=0.07, p=0.991; Fig. S4A).

To score shoaling tendency, we measured the distance between the live fish (Miller and Gerlai, 2012; Tunstrøm et al., 2013) (Fig. S4B). Control fish maintained an average distance of 7.098 cm. Average distances of 17.964 cm and 18.759 cm were registered for Match and Mismatch Chance pairs, respectively. Similar to the analysis of polarization, we determined that the distance between Control fish was smaller than the distance between Match and Mismatch pairs ($F_{2,18}$=48.96, p<0.001; p<0.05 in post-hoc tests; Fig. S4B) and that this effect was consistent over time ($F_{4,36}$=0.32, p=0.866; Fig. S4B).

Complementing the analysis of the temporal patterning of fish interactions, we assessed the extent to which behavioral teleporting maps the behavior of Control pairs onto the behavior of Match and Mismatch pairs. Such an assessment was performed through a further correlation analysis between schooling and shoaling. Once again, we focused on the time-intervals of Match and Mismatch conditions in which behavioral teleporting was successful (as determined in the main document). Chance values were calculated using fish from different trials of the Control condition, so that the Chance group consisted of 12 fish pairs of one small and one large animal, randomly selected from the Control condition. We utilized Matlab R2019b Statistics Toolbox and used the fitlm function to compute R^2 and the p-values. Predictably, schooling and shoaling patterns of Control pairs were significantly correlated (R^2=0.361, p<0.001; Fig. S5A), so that fish would tend to swim along the same direction when in close proximity. This association was preserved in the Match condition (R^2=0.044, p<0.001; Fig. S5B), but it was lost in the Mismatch condition (R^2=0.011, p=0.111; Fig. S5C). Further, the analysis on the values obtained by chance showed that this dependency does not exist between two random fish (R^2=0.006, p=0.161; Fig. S5D).

Overall, these findings suggest that live fish did not perceive the replicas as an attractive stimulus in comparison with other conspecifics. A possible explanation for this claim is that all the experimental fish were naïve to the replicas, whereby they were introduced to the stimulus for the first time during the trials, different from Control subjects that habituated to each other for two days in the same housing tank. It is tenable that 10 min of experimental time might not be sufficient to acclimate to a robotic stimulus. At the same time, behavioral teleporting was successful in selectively preserving the association between shoaling and schooling, whereby Match pairs were found to align their motion when swimming in close proximity to the replicas, similar to Control subjects swimming in the same tank.

Text S3. Fish body size, related to Figure 1

The selection of fish (small versus large) for the experiments was based on the measurement of their body size, which was conducted as follows. First, we gently hand-netted the fish from their collective housing tanks into a shallow plastic beaker filled with water. Then, we placed the beaker on top of a grid paper and took a high-resolution photo of the fish with an overhead camera (iPhone X, Apple, Cupertino, CA, USA). Once the photo was taken, the fish was placed back in the holding tank for the experiments. Using an open-source software (ImageJ, National Institute of Health, Bethesda, MD, USA), we measured the body length of the fish with respect to the millimeter scale of the grid paper. We obtained an average body length of 25.9 mm (25.2 mm) and 31.8 mm (36.0 mm) for small and large males (females), respectively. Across all pairs, large fish were 32.7% larger than small fish. Individual measurements of all the fish used in this study are reported in Table S1.

Text S4. Parametric study on transfer entropy, related to Table 1

Toward the rigorous application of transfer entropy to examine fish interaction, we conducted a parametric study to determine the optimal resolution that minimizes noise. Following standard practice (Bossomaier et

al., 2016), we computed entropy as a function of the sampling time ranging from 0.1 s to 1 s with a resolution of 0.05 s, and we chose the resolution at which entropy was minimized. The optimization was carried out on the symbolic time-series of all the animals across all conditions (a total of 72 time-series). The initial value of the sampling-time was based on the software and hardware constraints of the robotic platform, whereby the use of physically unrealistic sampling-times might beget false positive results (Weber et al., 2017). Results from the analysis indicate an optimal resolution of 0.1 s (Fig. S6A).

For the Control condition, interaction between two fish was assumed to be instantaneous between consecutive time-steps (Butail et al., 2016; Collignon et al., 2019; Strandburg-Peshkin et al., 2013). For the Match and Mismatch conditions instead, one should expect a time-delay in the interaction between the remotely-located animals. To determine such a delay, we evaluated the sum of the transfer entropy values from the small to the large fish and from the large to the small fish in the Match condition, for different time-delays varying from 0 to 4 time-steps (0 s to 0.4 s). The sum of the transfer entropy values is indicative of the overall strength of the interaction between the animals (Wibral et al., 2013). Although the dependence of the sum of the transfer entropies on the time-delay was minimal, a local peak corresponding to 0.2 s can be identified (Fig. S6B). This value of the time-delay was in agreement with our predictions, whereby we estimated a total time of 0.2 s for the simultaneous behavioral teleporting across the tanks. Hence, we used a delay of 0.2 s when scoring behavioral interactions in the Match and Mismatch conditions, with respect to both transfer entropy and cross-correlation analyses.

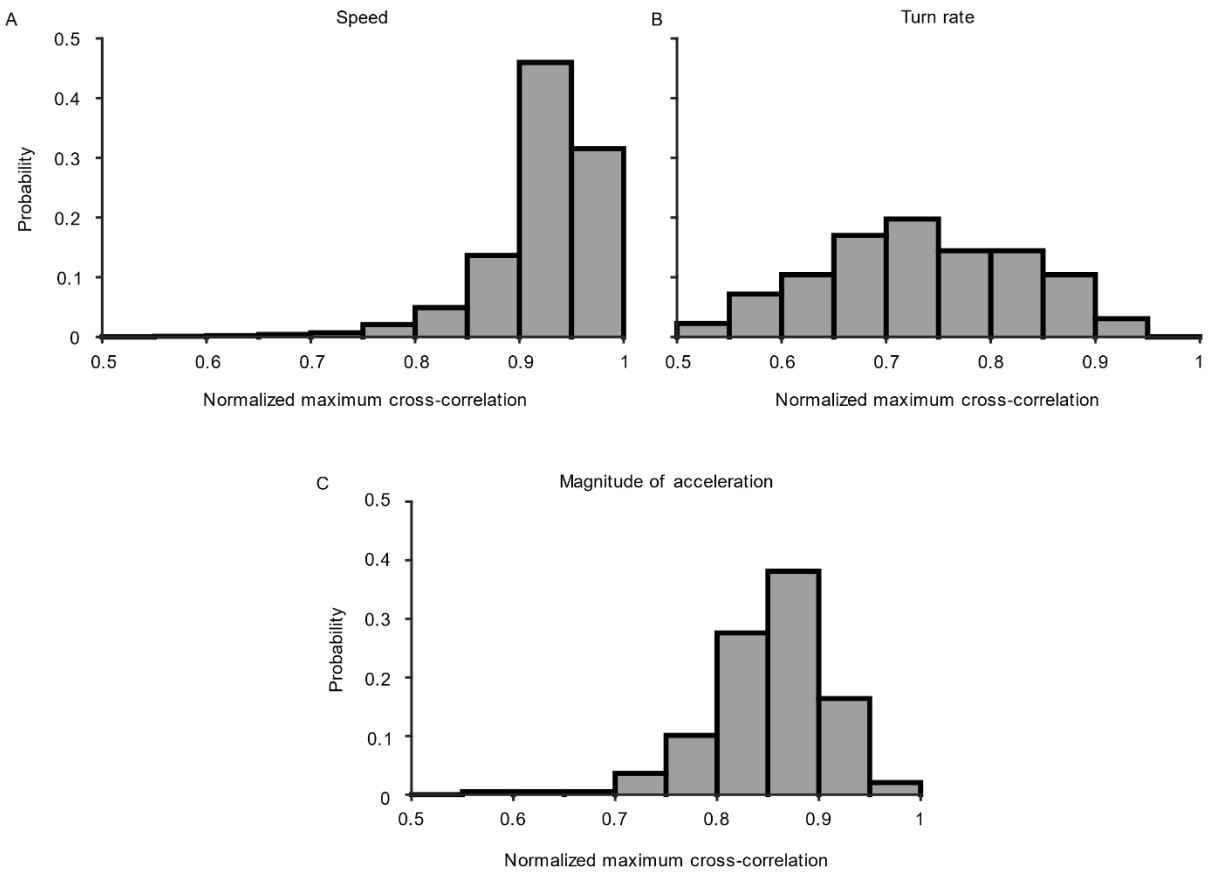

Figure S1. Additional performance analysis of the robotic platform, related to Figure 2. Histograms of normalized maximum cross-correlation between the robotic replica and the corresponding fish whose behavior is being teleported for all the acceptable trials. The analysis is conducted for three different metrics: **A**) speed, **B**) turn rate, and **C**) magnitude of the acceleration.

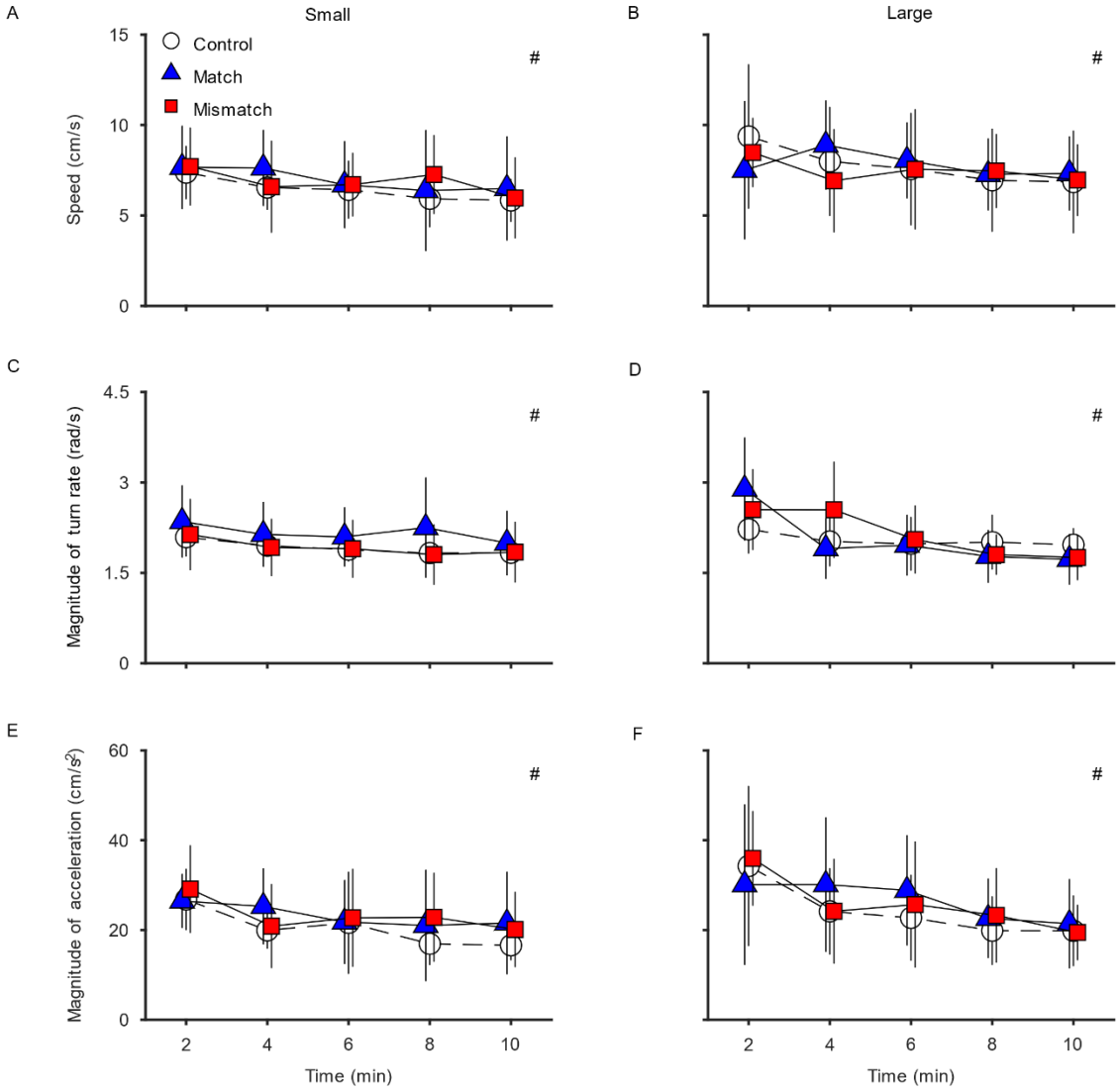

Figure S2. Temporal patterning of swimming activity of live fish, related to Figure 3 and Table 1. The analysis is conducted for: **A,B**) speed, **C,D**) magnitude of the turn rate, and **E,F**) magnitude of the acceleration, for **A,C,E**) small and **B,D,F**) large fish. White circles refer to Control condition, blue triangles to Match condition, and red squares to Mismatch condition. Data are expressed as means ± standard deviations. # indicates a significant time-effect at 5% significance level in post-hoc comparisons.

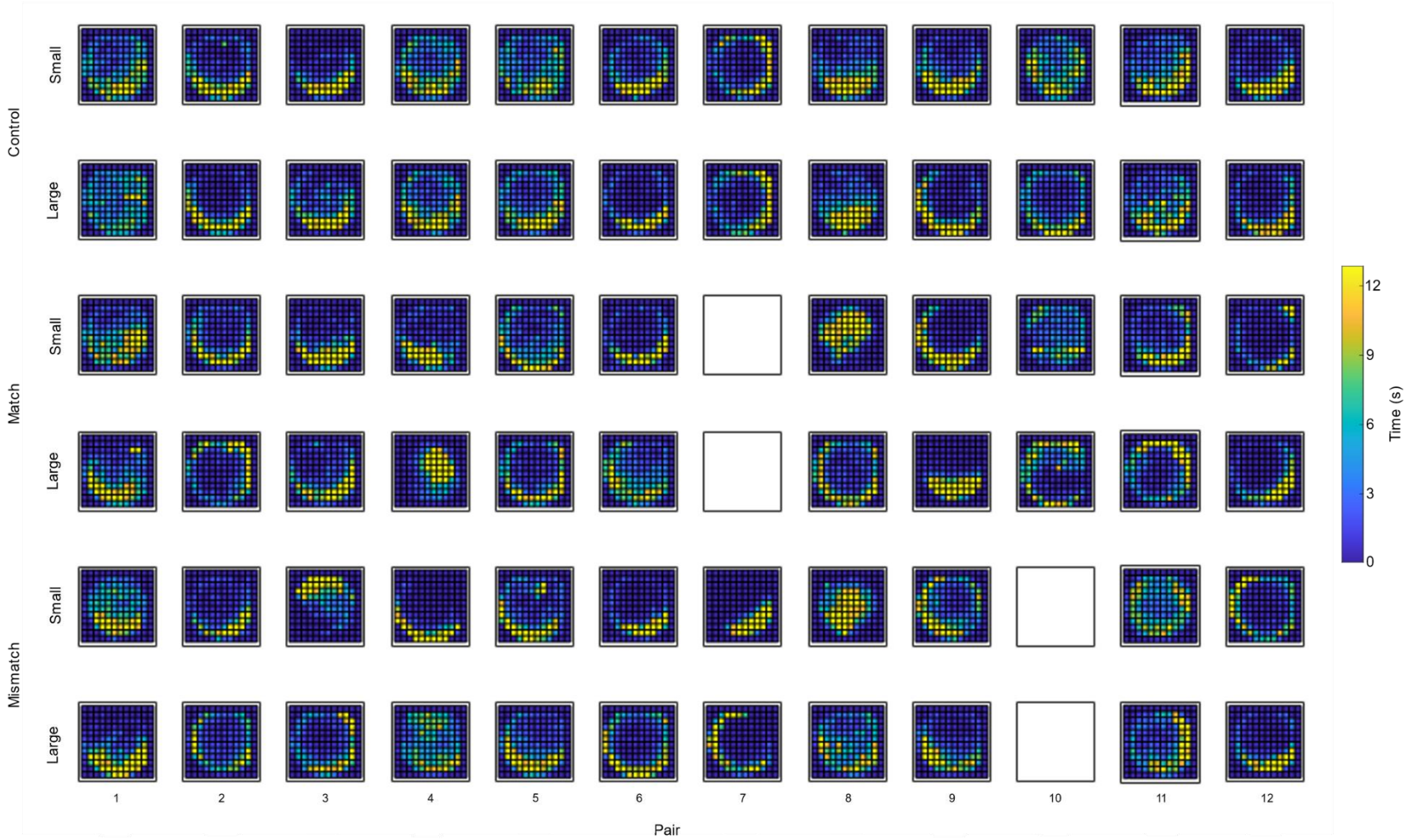

Figure S3. Spatial distribution across all experimental trials, related to Figure 3 and Table 1. The color indicates the time by each live fish in different portion of the experimental tank. Empty frames correspond to trials that were excluded from the analysis due to technical issue with the robotic platforms.

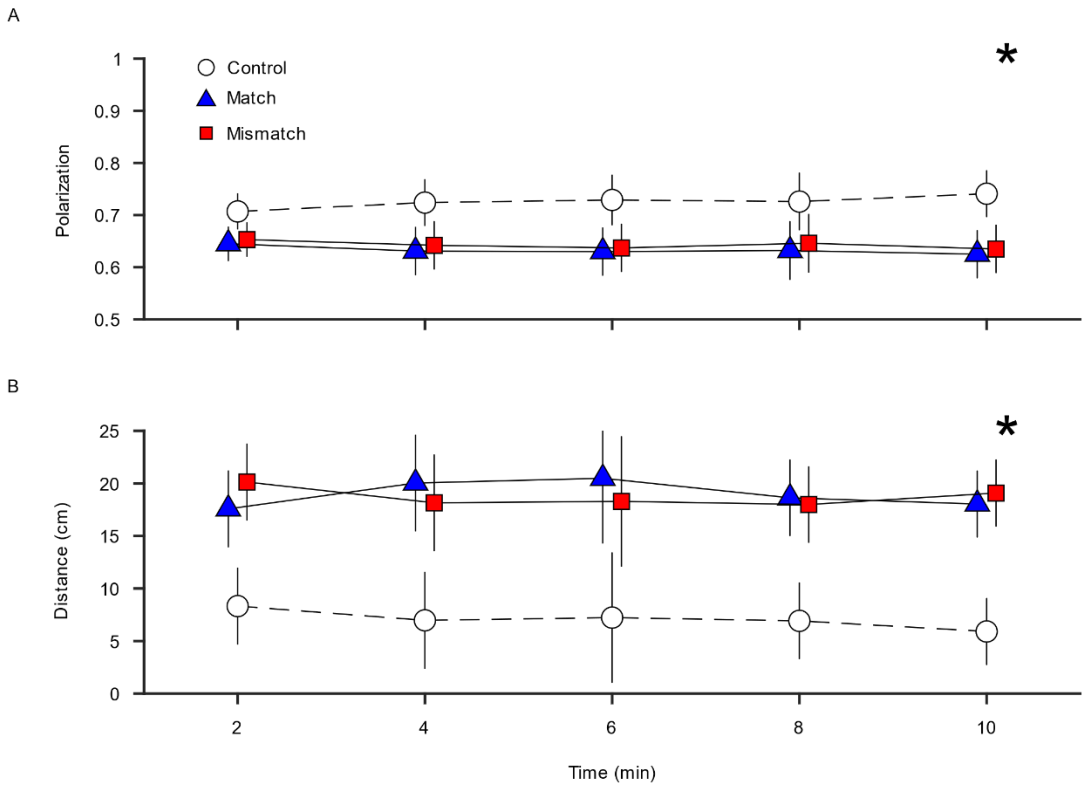

Figure S4. Temporal patterning of the interaction between two live animals, related to Figure 3 and Table 1. **A**) Polarization of the two live fish in a given pair, as a function of time and condition. **B**) Distance between two live fish in a given pair, as a function of time and condition. White circles refer to Control condition, blue triangles to Match condition, and red squares to Mismatch condition. Data are expressed as estimated marginal means ± standard deviations. * indicates $p<0.05$ in post-hoc comparisons between Match/Mismatch conditions and Control.

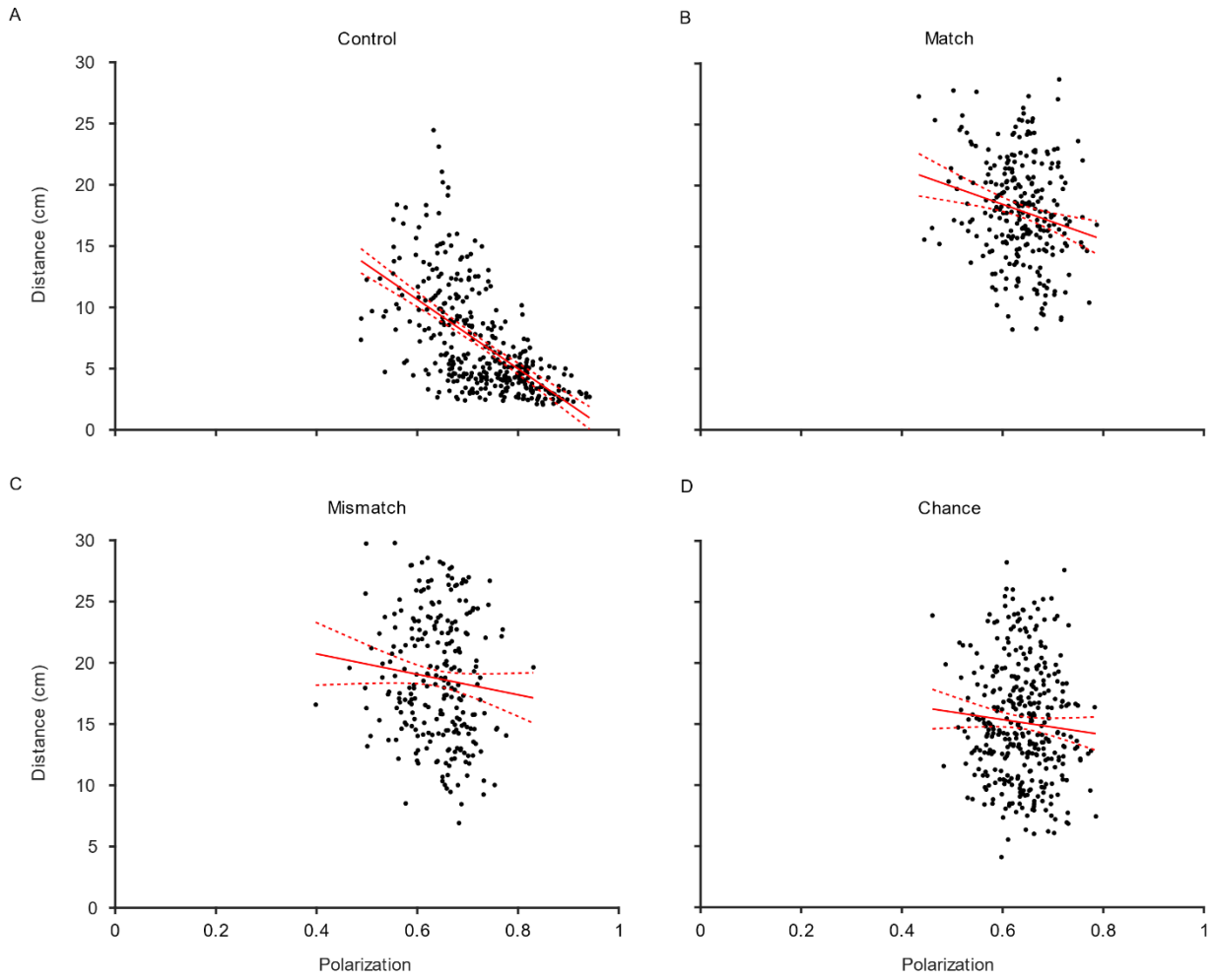

Figure S5. Correlation between shoaling and schooling, related to Figure 3 and Table 1. Linear regression analyses between the distance between two fish and their polarization. **A**) Control; **B**) Match; **C**) Mismatch; and **D**) Chance pairs. For the case of Match and Mismatch pairs, the calculation is limited to the time-intervals deemed successful in the similarity index analysis in. Black points are individual data points, solid red line is the linear regression line, and dashed red lines are the confidence intervals.

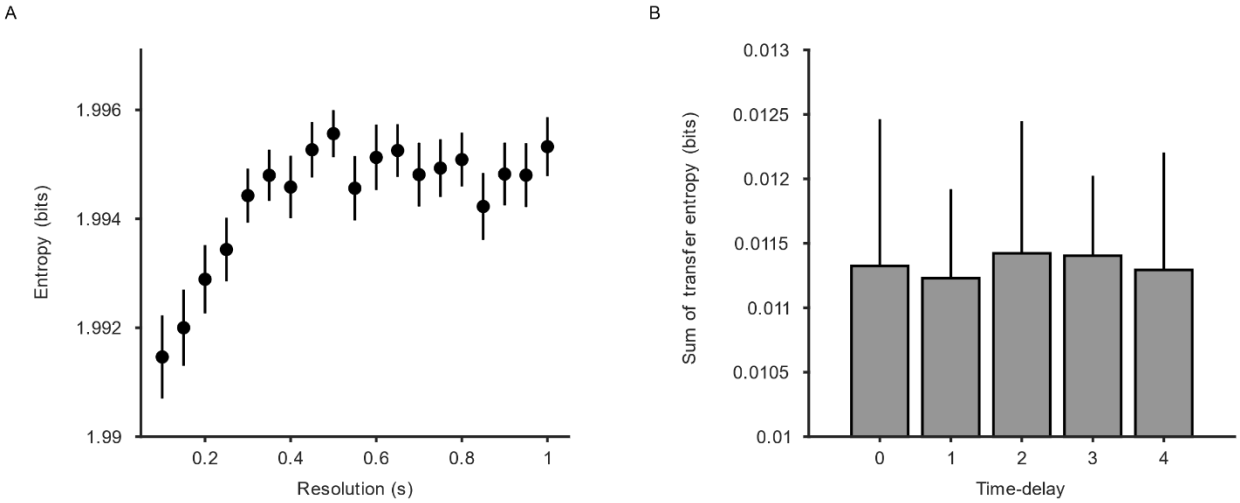

Figure S6. Parametric analysis for transfer entropy, related to Table 1. **A**) Downsampling analysis on the entropy of all the subjects to select the optimal resolution for transfer entropy computations; black dots are entropy values for a given resolution and lines are standard errors. **B**) Time-delay analysis for the Match condition to estimate the physical delay due to behavioral teleporting; lines represent standard error.

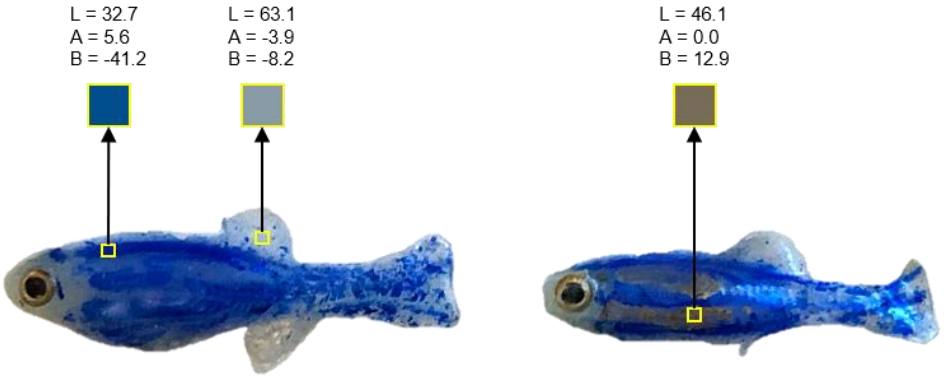

Figure S7. Color measurements of the replicas in CIELAB space from spectral analysis, related to Figure 1. The color of the stripe pattern of the replicas is shown in the left and right measurements, while the color of the silicone used for the mold is shown in the middle measurement. Left is a replica of a female subject and right is the replica of a male subject.

Pair	Large (mm)	Small (mm)
M-1	35.5	27.0
F-1	35.6	26.5
M-2	33.2	29.5
F-2	35.6	26.2
F-3	28.7	26.0
M-3	35.0	23.7
M-4	30.8	24.4
F-4	38.8	24.5
M-5	32.2	26.0
F-5	34.6	25.3
F-6	30.2	23.0
M-6	36.3	25.2

Table S1. Fish body size, related to Figure 1. Body size of all the experimental subjects employed in the study. “M” and “F” identify whether the pair is composed of male or female subjects, and the adjacent number labels the pair.

	Day 1		Day 2		Day 3	
Morning	M-1	Control	M-1	Match	M-1	Mismatch
	F-1	Control	F-1	Match	F-1	Mismatch
	M-2	Match	M-2	Mismatch	M-2	Control
	F-2	Match	F-2	Mismatch	F-2	Control
	F-3	Mismatch	F-3	Control	F-3	Match
	M-3	Mismatch	M-3	Control	M-3	Match
Afternoon	M-4	Control	M-4	Mismatch	M-4	Match
	F-4	Control	F-4	Mismatch	F-4	Match
	M-5	Match	M-5	Control	M-5	Mismatch
	F-5	Match	F-5	Control	F-5	Mismatch
	F-6	Mismatch	F-6	Match	F-6	Control
	M-6	Mismatch	M-6	Match	M-6	Control

Table S2. Counterbalancing procedure, related to Figure 1. Allocation, order of testing, and timing of experimental pairs to the three different conditions.

Transparent methods

Experimental setup

The experimental apparatus consisted of two cylindrical tanks on an elevated base, two robotic platforms, two webcams, and a desktop computer. The elevated base, made of aluminum T-slot bars (McMaster-Carr, Elmhurst IL) and a 6.3 mm thick plywood panel (60 cm × 120 cm, width × height; Home Depot, Atlanta GA), was placed at the center of the experimental area (Fig. 1A). Both manipulators were positioned side-by-side under the base. Two circular tanks (36 cm × 15 cm, diameter × depth) were placed on the base, centered with respect to the manipulators. Green tanks were chosen to confer a homogenous background for tracking and offer a less stressful environment for fish (Oliveira et al., 2015). Two 250 lumen LED lamps (Target, Minneapolis MN) were positioned 75 cm above the base to provide a uniform white background (ambient lighting: 200 lux). Two overhead cameras (Logitech C920 Pro, Logitech, Lausanne, Switzerland) were mounted 75 cm above the tanks to record the experiments, at a resolution of 640 × 360 pixels and an acquisition rate of 20 frames per second. The cameras and platforms were connected to an HP Z4-G4 workstation (HP, Palo Alto CA), which served the twofold purpose of: i) performing real-time tracking of live fish and replicas in both tanks, and ii) maneuvering each of the replicas to mirror the motion of the fish in the other tank.

Robotic platform and live tracking system

In order to maneuver the replicas along biologically relevant locomotory patterns through nonintrusive actuation, we used a custom-designed robotic manipulator (Fig. 1A). This device consisted of a two-dimensional Cartesian manipulator with two NEMA 17 stepper motors along each axis (MakeBlock XY Plotter, MakeBlock, Shenzhen China). The workspace of the Cartesian manipulator was 390 mm by 320 mm (length × width). A magnetic system was used to couple the end-effector with the replica, similar to other experimental setups in the literature (Bonnet et al., 2016; Landgraf et al., 2016; Romano et al., 2020). Specifically, a neodymium magnet (25.4 mm × 6.4 mm, diameter × thickness; McMaster-Carr, Elmhurst IL) was placed on a 3D-printed end-effector, which was tethered to the manipulator (Fig. 1A). Another magnet (6.4 mm × 6.4 mm, diameter × thickness; McMaster-Carr, Elmhurst IL) of opposite polarity was housed inside the replica such that it would be pulled along the paths traversed by the manipulator, without physical contact and at a minimal friction. Different from De Lellis et al. (2020), we did not include a dedicated motor for rotating the replica to reduce computational burden and mechanical noise in the tank.

The manipulator was driven by a microcontroller (Arduino Uno, Arduino, Italy), interfaced with a stepper motor shield (Kuman CNC Shield, Kuman, China) for signal generation/modulation and power supply. Closed-loop control was implemented through the Grbl(tm) v0.9 library (Jeon, 2011), a software for stepper motor control in Arduino. Use of stepper motors and low friction rails allowed an accurate position and velocity control without feedback, guaranteeing a resolution of 0.2 mm and a smooth motion of the end effector with minimum hysteresis.

We developed a tracking software to identify fish and replicas with high accuracy, while distinguishing their identities throughout the trial. Before each experimental session, the tracking software was initialized. During this phase, the robotic platform was calibrated using a homing sequence, where the end-effector was positioned at the center of the working space. Kalman predictors were reset and video writers were set-up. Next, the replica was magnetically connected to the end-effector.

Following the initialization phase, we cropped the video streams from the webcams into 400 × 400 pixel size, centering the experimental tanks in the images. From these cropped images, we manually identified a circular region of interest over the experimental area, and created a binary mask based on the selected region. The binary image frame aided in eliminating uncertainty due to external factors, such as lighting and shadows. To facilitate identification of the targets, we duplicated the masked frames and changed the image space of the duplicated image from red-green-blue (RGB) to hue-saturation-value (HSV). By applying image thresholds, we created two binary masks, which together served to identify both targets and keep their identities. From the saturation and value layers, we identified the two targets against the homogeneously illuminated background in the experimental region. To resolve the identity of the replica

from the fish, we used the hue layer, from which we identified the blue pigment of the silicone replica (not present in the live fish).

Toward ultimately determining the location of the two targets, we used a blob analyzer in Matlab R2019b (Mathworks MA, USA). The blob analyzer recognized connected pixels in the binary masks, from which we inferred the location of a target as the centroid of the corresponding blob. To improve on the resolution of the identities during potential occlusions, we filtered instances in which the fish centroid was closer than 20 pixels to the replica centroid. A Kalman predictor was then used to solve these instances. The predictor used the position of the two targets prior to the potential occlusion, assuming their velocities were constant (Blackman, 1986). The confidence values between the Kalman predictions and all the detected objects were calculated to generate a cost matrix, which was employed to identify the most probable object locations through Munkres' assignment algorithm (Munkres, 1957).

Once the centroid positions were identified, the position of each fish was transferred to the replica in the opposite tank, thereby affording behavioral teleporting of fish motion. The overall delay in transferring fish motion to the replica was approximately 40 ms: 10 ms was the time required to analyze images in each tank and 30 ms was the communication cycle of each microcontroller. Therefore, to minimize delay and interference of data transfer between the microcontrollers, we updated the positions of the replicas every 100 ms. We minimized confounds associated with fish tracking uncertainty, by averaging the position of the fish in the previous and current frames before sending the command to the microcontrollers. Due to physical limitations of the stepper motors, the maximum speed of the replicas was set at 20 cm/s, so that a single position update would consist of a motion of at most 2 cm.

Replica

To investigate the interaction between robots and live fish, we designed a conspecific-like replica based on a live zebrafish (*Danio rerio*) (De Lellis et al., 2020). We tested four different replicas, whose dimensions were based on the average size of experimental fish: a small male (26 mm in length), large male (32 mm in length), small female (25 mm in length), and large female (36 mm in length) (Fig. 1B) (Supplemental Information: Text S3 and Table S1).

The replicas were created in skin-safe silicone (Dragon Skin 10, Smooth – On, USA), toward a soft body capable of undulating during maneuvers, similar to previous studies (Bonnet et al., 2016; De Lellis et al., 2020; Romano et al., 2019). The original three-dimensional computer-aided-design (CAD) of a zebrafish developed by Kim et al. (2018) was used as a reference to create the four replicas. Specifically, by tailoring the morphology of the original model according to acquired pictures of live animals, we 3D-printed four rigid models in polylactic acid (PLA) filament using a MakerBot Replicator 5 (MakerBot, New York, NY, USA). Then, the molds for the four silicone replicas were produced from polyethylene terephthalate glycol (PETG) using a vacuum forming machine over the 3D-printed models. Molds were filled with skin-safe silicone (Dragon Skin 10, Smooth – On, USA) to create replicas, which were painted with non-toxic acrylic paint (Smooth – On, USA).

We painted the replicas using silicone pigments and silver specks, following natural coloration patterns (males in gold and blue patterns, and females in silver and blue patterns). The coloration patterns of the replicas in CIELAB color space were measured using a spectrometer (USB2000, Ocean Optics, FL, USA), similar to (Romano et al., 2020) (Supplemental Information: Fig. S7). To improve the realism of replicas, two glass eyes (Van Dyke Supply Co., Granite Quarry, NC, USA) were glued onto the replicas (Landgraf et al., 2016). Finally, a 0.75 mm diameter wire was inserted through the middle of the replica to create a spine that would provide a mechanical connection to the magnetic base.

The base to which the replica was tethered comprised a plastic shaft and a magnetic attachment. The plastic shaft consisted of a 4 cm hollow conical body, through which the wire extending from the replica spine was inserted. The wire was free to rotate around its axis in the shaft, allowing the replica to passively align itself with the swimming direction. The plastic shaft was glued to a 3D-printed support, housing the magnet.

Experimental procedure

Adult wild-type zebrafish were purchased from Carolina Biological Supply (Burlington NC, USA). Upon delivery, all animals were allowed for an acclimation period of at least 14 days to the laboratory conditions. Photos of individual fish were taken on a millimeter paper background to measure their body length. We formed pairs of the same sex, with a small and a large fish. Each pair was housed in a separate tank for a two-day habituation period (Supplemental Information: Table S1), and each pair was tested in all three conditions in a counterbalanced order over three consecutive days (Supplemental Information: Table S2). All animals were kept under a 12 hour light-dark cycle, with lights on at 9:00 AM at an intensity range between 50 and 100 Lux. Water temperature was maintained at 26ºC. In total, we tested 12 male and 12 female fish.

Before each of the two daily experimental sessions (morning and afternoon), the tanks were washed and filled with 26ºC water up to 6 cm in depth. Six male and six female pairs were tested for three conditions, namely: “Control,” “Match,” and “Mismatch” (Fig. 1C). These conditions were designed to investigate the effect of body size and associated locomotory patterns on leadership. In the Control condition, both fish were allowed to swim in the same tank (Supplemental Information: Video S1). In the Match condition, a small fish swam in a tank with a large replica that replicated the motion of a large fish, which was swimming in the other tank with a small replica that, in turn, replicated the motion of the small fish (Supplemental Information: Video S2). The Match condition aimed at testing whether transferring information from a live individual to robotic replica would preserve the interaction between the live fish observed in the Control condition (a large and a small fish of the same sex swimming together). Should the replicas be appraised as conspecifics, the Match condition would result in a remote interaction between fish in different tanks analogous to the interaction between fish in the same tank of the Control condition. In the Mismatch condition, a small fish swam in a tank with a small replica that replicated the motion of a large fish, which was swimming in the other tank with a large replica that, in turn, replicated the motion of the small fish (Supplemental Information: Video S3). The Mismatch condition was intended to decouple body size from locomotory patterns, thereby introducing a manipulation in the remote interaction between fish.

At the beginning of each experiment, each of the fish in the pair was placed in a separate opaque cylinder in the experimental tanks and allowed to habituate to the water temperature for ten minutes. At the end of the habituation phase, the cylinders were lifted, and the manipulators and cameras were turned on. After ten minutes of experiment, the fish were placed back into their housing tanks in pairs.

Data analysis

Data were analyzed using the statistical toolbox in Matlab R2019b. First, the trajectories obtained from live tracking at a sampling rate of 20 frames per second were smoothed using a Gaussian weighted moving average over a 0.5 s window. To quantify the ability of the replicas to mirror the motion of the fish, we introduced a similarity index as a normalized two-dimensional cross-correlation of the trajectories of the replica and the corresponding live fish in the opposite tank (Fig. 2A). First, we divided the data into time-intervals of 20-s with a total of n=400 data points. Then, cross-correlation between the position of the replica and the fish over the k-th time-interval (each of 20-s) at a time-lag of τ time-steps (each of 0.05 s in duration) was computed as (Buck, 2002)

$$C(\tau,k)=\sum_{t=1}^{n-\tau} R(t+\tau+(k-1)n)\cdot F(t+(k-1)n)$$

,

where a dot is used to indicate inner product between the two-dimensional position of the replica and the fish, R and F. The computed cross-correlation value was normalized by the autocorrelation of each process through

$$\hat{C}(\tau,k)=\frac{C(\tau,k)}{\sqrt{\sum_{t=1}^{n}\|R(t+(k-1)n)\|^2}\sqrt{\sum_{t=1}^{n}\|F(t+(k-1)n)\|^2}}$$

where we have used $\|\cdot\|$ to identify the Euclidean norm of a vector. The normalized cross-correlation ranges between 0 and 1, with 1 corresponding to the replica exactly mirroring the two-dimensional position of the fish at a time-lag τ for the entire duration of the k-th time-interval.

By maximizing the normalized cross-correlation as a function of the time-lag, we gathered information regarding the physical delay in transferring information between the tanks. At the same time, the corresponding value of the maximum normalized cross-correlation is indicative of the accuracy of the robotic platform in replicating the motion of a live animal. Hence, we defined a similarity index as the maximum value of the normalized cross-correlation and we retained the time-lag at which such a maximum was attained for all the considered time-intervals. We deemed successful the trials in which the average similarity index was more than 0.95 and the average time-lag at which the cross-correlation was maximized was less than 0.2 s, for both the instances of behavioral teleporting that were conducted in parallel in the two tanks. Each experimental trial consisted of thirty time-intervals of 20 s. Based on the similarity index results, we identified two trials, one for Match and one for Mismatch conditions, where the replicas failed to replicate (similarity index below 95% within a time-lag of up to 0.2 s) fish motion for more than 70% of the time-intervals. Excluding these two trials, the robotic replicas were successful in replicating fish motion in 85% of the experimental time (Fig. 2B).

Building on our previous work (Porfiri, 2018), we used information-theoretic methods to determine influence between small and large zebrafish. Transfer entropy measures the reduction of the uncertainty in the prediction of the future of a dynamical system from its past, given additional information regarding the past of another dynamical system. A non-zero transfer entropy value points at a possible causal influence of a dynamical system on another in a Wiener-Granger sense (Bossomaier et al., 2016).

To score transfer entropy between the fish, we employed a symbolic approach (Porfiri, 2018), where the time-series of the fish were mapped to discrete symbols. First, we down-sampled the time-series of speed and turn rate of each fish at 10 Hz, to reduce the effect of noise, following standard practice in transfer entropy analysis (Porfiri, 2018) (Supplemental Information: Text S4 and Fig. S6). Speed was measured as the magnitude of the first-order numerical derivative of the position obtained from tracking, and turn rate was calculated with a finite difference approximation of the curvature of the trajectory. Then, we jointly symbolized the time-series based on ordinal patterns, which would encapsulate a simplified ethogram of each animal. For each time-series, we used binary symbols, associated with increasing and decreasing trends of consecutive values (Fig. 4A,B). Then, we merged the two time-series of binary symbols into one time-series of four possible symbols, each representing a combination of increasing/decreasing trend in speed and turn rate (Fig. 4C).

We computed the transfer entropy from small to large fish at a given delay of τ time-steps (each of 0.1 s in duration) as follows:

$$\mathrm{TE}_{\mathrm{Small}\rightarrow\mathrm{Large}} = \sum_{L(t+1),L(t),S(t-\tau)} \Pr(L(t+1),L(t),S(t-\tau))\log_2 \frac{\Pr(L(t+1)|L(t),S(t-\tau))}{\Pr(L(t+1)|L(t))}$$

where L and S are the symbolized time-series for large and small fish, "Pr" is the probability mass function computed with a plug-in estimation, over the 20-s time-intervals where the similarity index was above 0.95 for a time-lag less than 0.2 s, and τ is the delay. No time-delay was used for the Control condition as the two fish interacted in real time, and a time-delay of 0.2 s ($\tau = 2$) was used for the Match and Mismatch conditions, to account for the physical delays in replicating the motion of a fish on the replica in the opposite tank (Supplemental Information: Text S4 and Fig. S6). Transfer entropy from large to small fish was computed by simply exchanging L and S the equation above.

We scored the significance of the information transfer using a permutation test (Nichols and Holmes, 2002). More specifically, we computed transfer entropy values between all possible shuffling of trials (*N)* of a condition. From this *N* × *N* matrix, *N* transfer entropy values were randomly selected, and their average values were recorded. This process was repeated for a total of 20,000 times to create a surrogate distribution, which was used to test the null hypothesis. To infer an influence through transfer entropy, we statistically tested true transfer entropy values against the surrogate distribution with a permutation test at 5% significance level.

Cross-correlation analysis was used as an additional measure to further investigate leadership within the pair, thereby isolating whether a fish would tend to initiate maneuvers that will be followed by the other (Krause et al., 2000). First, the speed and turn rate of live fish were down-sampled to 10 Hz, similar to the transfer entropy analysis. Then, we calculated the maximum cross-correlation and corresponding time-lag for both speed and turn rates of two live fish over the 20-s time-intervals with similarity scores above 0.95 for a time-lag less than 0.2 s, independently. We adapted the formula for the similarity index, by simply using one-dimensional time-series (speed or turn rate) of the two fish in place of the two-dimensional position data of the fish and replica. In this vein, a large value of the maximum normalized cross-correlation of any of these two metrics would identify coordination between the fish and the sign of the corresponding time-lag would reveal which fish acts as a leader. Similar to the transfer entropy analysis, the time-series for Match and Mismatch conditions were offset of 0.2 s to account for the platform delay. For example, a time-lag of 0.1 s from small to large fish in Match condition would mean that the small fish led the large fish by 0.3 s. We created a surrogate dataset for each of the metric (maximum value of normalized cross-correlation and corresponding time-lag for both speed and turn rate) by using the same approach as described for transfer entropy, and we analogously assessed statistical significance using a permutation test at 5% significance level.

Ethics statement

All animal procedures were approved by the University Animal Welfare Committee of New York University under protocol number 13-1424.

Supplemental references

Blackman, S.S. (1986). Multi-target tracking with radar applications (Dedham, MA: Artech House, Inc.).

Bonnet, F., Kato, Y., Halloy, J., and Mondada, F. (2016). Infiltrating the zebrafish swarm: design, implementation and experimental tests of a miniature robotic fish lure for fish–robot interaction studies. Artificial Life and Robotics *21*, 239-246.

Bossomaier, T., Barnett, L., Harré, M., and Lizier, J.T. (2016). An introduction to transfer entropy. Cham: Springer International Publishing, 65-95.

Buck, J.R. (2002). Computer explorations in signals and systems using MATLAB, 2nd edn (Upper Saddle River, N.J. :: Prentice Hall).

Butail, S., Mwaffo, V., and Porfiri, M. (2016). Model-free information-theoretic approach to infer leadership in pairs of zebrafish. Physical Review E *93*, 1-12.

Collignon, B., Séguret, A., Chemtob, Y., Cazenille, L., and Halloy, J. (2019). Collective departures and leadership in zebrafish. PLoS ONE *14*, 1-16.

De Lellis, P., Cadolini, E., Croce, A., Yang, Y., di Bernardo, M., and Porfiri, M. (2020). Model-based feedback control of live zebrafish behavior via interaction with a robotic replica. IEEE Transactions on Robotics *36*, 28-41.

Jeon, S.K. (2011). An open source, embedded, high performance g-code-parser and CNC milling controller written in optimized C that will run on a straight Arduino (GitHub).

Kim, C., Ruberto, T., Phamduy, P., and Porfiri, M. (2018). Closed-loop control of zebrafish behaviour in three dimensions using a robotic stimulus. Scientific Reports *8*, 657-657.

Krause, J., Hoare, D., Krause, S., Hemelrijk, C., and Rubenstein, D. (2000). Leadership in fish shoals. Fish and Fisheries *1*, 82-89.

Landgraf, T., Bierbach, D., Nguyen, H., Muggelberg, N., Romanczuk, P., and Krause, J. (2016). RoboFish: Increased acceptance of interactive robotic fish with realistic eyes and natural motion patterns by live Trinidadian guppies. Bioinspiration and Biomimetics *11*.

Miller, N., and Gerlai, R. (2012). From schooling to shoaling: patterns of collective motion in zebrafish (*Danio rerio*). PLoS ONE *7*, e48865.

Munkres, J. (1957). Algorithms for the assignment and transportation problems. Journal of the Society for Industrial and Applied Mathematics *5*, 32-38.

Nichols, T.E., and Holmes, A.P. (2002). Nonparametric permutation tests for functional neuroimaging: A primer with examples. Human Brain Mapping *15*, 1-25.

Oliveira, J., Silveira, M., Chacon, D., and Luchiari, A. (2015). The zebrafish world of colors and shapes: preference and discrimination. Zebrafish *12*, 166-173.

Porfiri, M. (2018). Inferring causal relationships in zebrafish-robot interactions through transfer entropy: a small lure to catch a big fish. Animal Behavior and Cognition *5*, 341-367.

Romano, D., Benelli, G., Hwang, J.-S., and Stefanini, C. (2019). Fighting fish love robots: mate discrimination in males of a highly territorial fish by using female-mimicking robotic cues. Hydrobiologia *833*, 185-196.

Romano, D., Elayan, H., Benelli, G., and Stefanini, C. (2020). Together We Stand–Analyzing Schooling Behavior in Naive Newborn Guppies through Biorobotic Predators. Journal of Bionic Engineering *17*, 174-184.

Strandburg-Peshkin, A., Twomey, C.R., Bode, N.W., Kao, A.B., Katz, Y., Ioannou, C.C., Rosenthal, S.B., Torney, C.J., Wu, H.S., Levin, S.A*., et al.* (2013). Visual sensory networks and effective information transfer in animal groups. Current Biology *23*, R709-R711.

Tunstrøm, K., Katz, Y., Ioannou, C.C., Huepe, C., Lutz, M.J., and Couzin, I.D. (2013). Collective states, multistability and transitional behavior in schooling fish. PLoS Computational Biology *9*, e1002915.

Weber, I., Florin, E., Von Papen, M., and Timmermann, L. (2017). The influence of filtering and downsampling on the estimation of transfer entropy. PLoS ONE *12*, e0188210.

Wibral, M., Pampu, N., Priesemann, V., Siebenhühner, F., Seiwert, H., Lindner, M., Lizier, J.T., and Vicente, R. (2013). Measuring information-transfer delays. PLoS ONE *8*, e55809.